

ATMOSPHERIC TURBULENCE EFFECTS  
ON LASER COMMUNICATIONS SYSTEMS

Tadd Edward Spicer

DUDLEY KNOX LIBRARY  
NAVAL POSTGRADUATE SCHOOL  
MONTEREY, CALIFORNIA 93940

# NAVAL POSTGRADUATE SCHOOL

## Monterey, California



# THESIS

ATMOSPHERIC TURBULENCE EFFECTS  
ON LASER COMMUNICATIONS SYSTEMS

by

Tadd Edward Spicer

December 1974

Thesis Advisor:

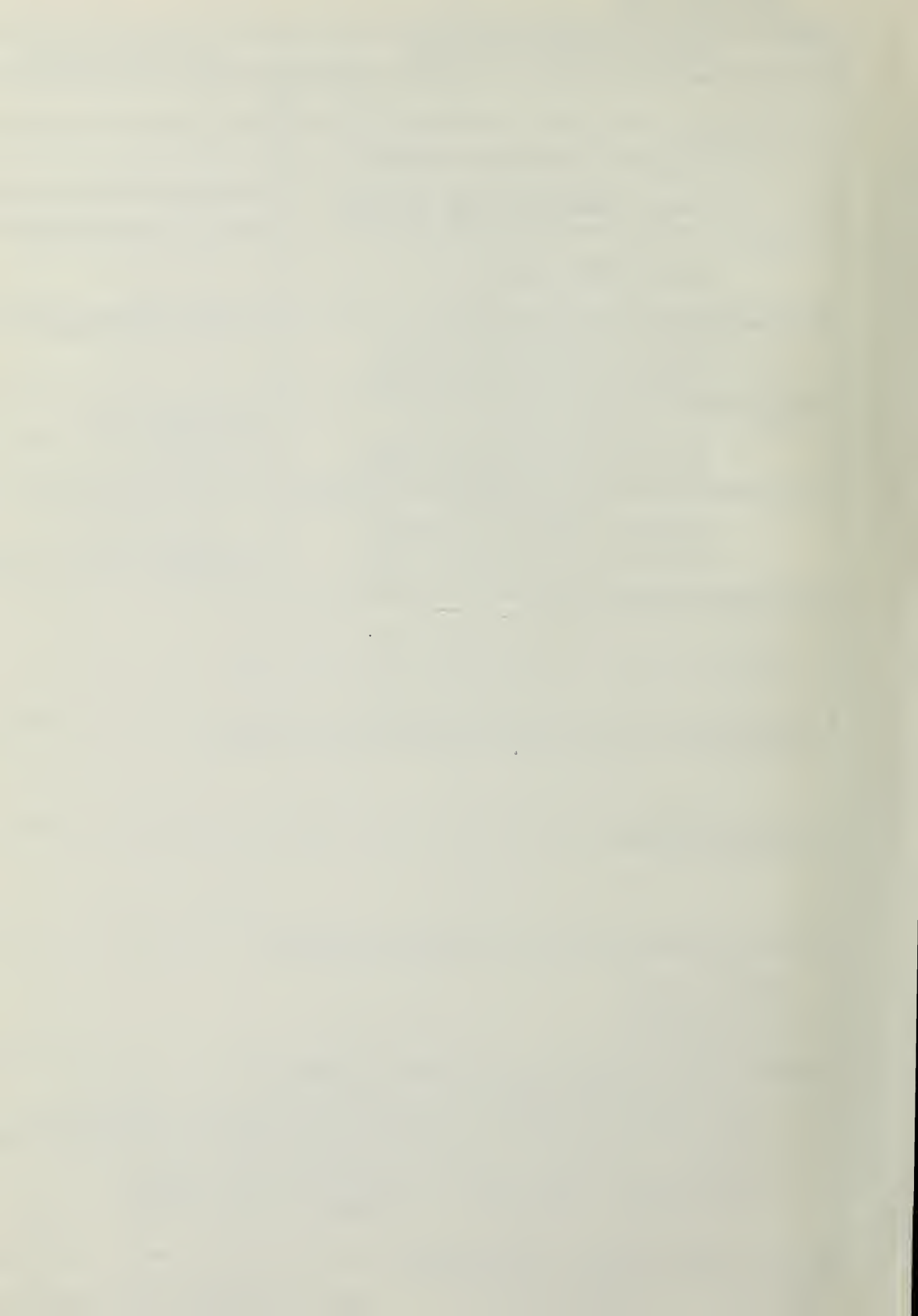
C.H. Rothage

Approved for public release; distribution unlimited.

T 1643



REPORT DOCUMENTATION PAGE		READ INSTRUCTIONS BEFORE COMPLETING FORM
1. REPORT NUMBER	2. GOVT ACCESSION NO.	3. RECIPIENT'S CATALOG NUMBER
4. TITLE (and Subtitle) Atmospheric Turbulence Effects on Laser Communications Systems		5. TYPE OF REPORT & PERIOD COVERED
7. AUTHOR(s) Tadd Edward Spicer		6. PERFORMING ORG. REPORT NUMBER
9. PERFORMING ORGANIZATION NAME AND ADDRESS Naval Postgraduate School Monterey, California 93940		8. CONTRACT OR GRANT NUMBER(s)
11. CONTROLLING OFFICE NAME AND ADDRESS Naval Postgraduate School Monterey, California 93940		10. PROGRAM ELEMENT, PROJECT, TASK AREA & WORK UNIT NUMBERS
14. MONITORING AGENCY NAME & ADDRESS (if different from Controlling Office) Naval Postgraduate School Monterey, California 93940		12. REPORT DATE December 1974
		13. NUMBER OF PAGES 61
		15. SECURITY CLASS. (of this report) Unclassified
		15a. DECLASSIFICATION/DOWNGRADING SCHEDULE
16. DISTRIBUTION STATEMENT (of this Report)  Approved for public release; distribution unlimited.		
17. DISTRIBUTION STATEMENT (of the abstract entered in Block 20, if different from Report)		
18. SUPPLEMENTARY NOTES		
19. KEY WORDS (Continue on reverse side if necessary and identify by block number) laser propagation scintillation modulation turbulence		
20. ABSTRACT (Continue on reverse side if necessary and identify by block number)  A multiplicative model for the prediction of frequency translation effects of scintillation caused by atmospheric turbulence on a simple intensity modulated laser communication system is tested. A revised experimental procedure is implemented. Some data is examined which suggests inadequacies in the model in regard to the prediction of		



the bandwidth of the translated scintillation noise. In general, the observed bandwidth of the translated scintillation noise is less than predicted by the model, however, frequency translation effects are readily apparent.







Atmospheric Turbulence Effects  
on Laser Communications Systems

by

Tadd Edward Spicer  
Lieutenant, United States Navy  
B.A., Northwestern University, 1966

Submitted in partial fulfillment of the  
requirements for the degree of

Master of Science in Electrical Engineering

from the

Naval Postgraduate School

December 1974



## ABSTRACT

A multiplicative model for the prediction of frequency translation effects of scintillation caused by atmospheric turbulence on a simple intensity modulated laser communication system is tested. A revised experimental procedure is implemented. Some data is examined which suggests inadequacies in the model in regard to the prediction of the bandwidth of the translated scintillation noise. In general, the observed bandwidth of the translated scintillation noise is less than predicted by the model, however, frequency translation effects are readily apparent.



## TABLE OF CONTENTS

I.	INTRODUCTION. . . . .	4
II.	BACKGROUND. . . . .	5
III.	THEORY REVIEW . . . . .	6
IV.	EXPERIMENTAL PROCEDURE. . . . .	9
	A. BASIC EXPERIMENT. . . . .	9
	B. REVISED EXPERIMENT. . . . .	11
	C. EQUIPMENT DESCRIPTION . . . . .	14
	D. OPTICAL RECEIVER SENSITIVITY. . . . .	18
	E. TAPE RECORDER NOISE . . . . .	20
V.	DATA DESCRIPTION AND ANALYSIS . . . . .	23
	A. DATA FORMAT AND REDUCTION TECHNIQUE . . . . .	23
	B. NOISE/INTERFERENCE. . . . .	24
	C. SCINTILLATION SPECTRUM. . . . .	27
	D. SPECTRUM OF MODULATED LASER . . . . .	38
VI.	CONCLUSIONS . . . . .	58
	LIST OF REFERENCES. . . . .	60
	INITIAL DISTRIBUTION LIST. . . . .	61



## I. INTRODUCTION

Laser communications systems, while still in their infancy, offer several inherent advantages over other types of communications links. Extremely wide bandwidths permit very high data rates to be used ( $10^{14}$  bits/sec are within the state of the art!) and the highly directional nature of the laser provides a security over and above that which may be readily provided by cryptographic protection of the information carried by the laser communications link.

The communications channel, or medium through which the laser system must operate, is the atmosphere. Propagation of a laser beam through the atmosphere is at best an uncertain operation. Refraction of the beam by both small and large scale changes in the index of refraction and attenuation due to absorption and scattering play a major role. Atmospheric turbulence is the primary cause of the refractive effects while precipitation and the presence of particulate matter in the atmosphere account primarily for the attenuation losses.

This work was a continuation of earlier work by Rankin (Ref.1) which had as its objective the examination of the effect of turbulence caused by small scale variations in the index of refraction which result in scintillation of the laser beam. The scope of this work was to examine in detail the scintillation effects on an intensity modulated laser beam, using the experimental procedure developed by Rankin. A brief review of the applicable theory is presented, but the major thrust of this report is a complete description of the experimental procedure and an examination of some data.





## II. BACKGROUND

This work was initially ~~done~~ in conjunction with an atmospheric laser propagation project conducted by Dr. Eugene Crittendon of the Naval Postgraduate School. The project studied small scale turbulence in the atmosphere at sea level in relation to scintillation and beam wander effects on Helium-Neon and CO<sub>2</sub> laser beams propagated between the Naval Postgraduate School Research Vessel Acania and a mobile shore facility. It was intended that the Helium-Neon laser could be modulated during the course of the data collection effort, allowing the collection of data on the effects of scintillation on an intensity modulated laser. However, compatibility problems between Dr. Crittenden's project and the needs of the modulated laser experiment forced a separation from the larger project and an independent data collection effort. A more detailed explanation is contained in Chapter 14.

Rankin (Ref. 1) initiated the work, established the basic data collection procedure, and obtained preliminary data. In this continuation, the data collection method has been refined and more extensive data taken.



### III. THEORY REVIEW

Turbulence of the atmosphere causes scintillation of a laser beam and scintillation, in turn, has a marked effect on information retrieval from intensity modulated laser communications systems. The theory underlying this chain of cause and effect is treated in detail in References 2,3,4,5, and 6, and only a brief qualitative discussion is included in this report.

The atmosphere, the medium through which the laser beam must of necessity pass, is constantly in motion. This motion is called turbulence. Wind, weather, heat, etc. are inextricably bound up with turbulence to the point where it is often difficult to distinguish cause from result. The final result, however, is that turbulence exists over a broad scale, from large movements of air masses to extremely small scale motion of air molecules, causing small scale fluctuations of pressure and temperature, which, in turn, cause random fluctuations in the index of refraction of the atmosphere.

A smooth and featureless optical wave or beam traversing this turbulent medium for more than a few meters has its energy redistributed and exhibits spatial fluctuations in intensity commonly known as "scintillation". Thus, stars appear to twinkle and distant lights appear to quiver. The logarithm of the intensity of the distorted wave has a Normal (Gaussian) probability distribution function, hence the magnitude of the intensity fluctuations is often referred



to as "log-intensity variance". The magnitude of the intensity fluctuations increases with the strength of the turbulence and with the length of time the beam is subjected to the turbulence, i.e. the path length. Over 'long enough' path lengths, saturation occurs and the magnitude of the fluctuations levels off. For paths close to the earth's surface, saturation can occur in a path length of a kilometer or so. The actual mechanism of scintillation is, of course, that the small scale random fluctuations in the index of refraction of the medium cause localized random refractions of the light beam. The actual appearance of scintillations in a laser beam can be readily observed by allowing the beam to fall on any opaque surface. The spatial and temporal fluctuations in the intensity are easily seen and have an appearance similar to the effect one sees when looking at the bottom of a swimming pool filled with water.

Thus scintillation of a laser beam is random intensity fluctuations which constitute an intensity modulation at frequencies nominally from D.C. to 300 Hz. or so, however, the high frequency limit is greatly dependent on the strength of the turbulence. (Scintillation out to about 1000 Hz was observed in the collection of data for this work.)

If the laser beam traversing this turbulent medium and being scintillated is itself intensity modulated with some type of waveform to convey intelligence, the scintillations interact with the intelligence in a multiplicative manner





with the effect that the low frequency scintillation noise is translated in frequency ~~and~~ noise sidebands about the intelligence modulation. Rankin (Ref. 1), using an intuitive approach, modelled the detector output to be of the form

$$M(t, S(t)) = [A + B \cos(\omega_m t + \theta)] [S_0 + S(t)]$$

where A is the D.C. level of the amplitude, B represents the percent modulation,  $\theta$  is a uniformly distributed random variable (phase shift),  $S_0$  is the D.C. level of the scintillation noise, and  $S(t)$  is a random process, independent of  $\theta$ , which describes the atmospheric scintillation. Then, by taking the Fourier Transform of the auto-correlation function of  $M(t, S(t))$ , the power spectral density ( $\phi_m$ ) of the signal plus scintillation noise at the detector output is

$$\begin{aligned} \phi_m(\omega) = & \frac{S_0^2 A^2}{2} + \frac{S_0^2 B^2}{2} [\delta(\omega - \omega_m) + \delta(\omega + \omega_m)] + \frac{A^2}{2} \phi_S(\omega) \\ & + \frac{S_0^2 B^2}{2} [\phi_S(\omega - \omega_m) + \phi_S(\omega + \omega_m)] \end{aligned}$$

where  $\phi_S(\omega)$  is the power spectral density of the scintillation alone.

The fourth term of equation (2) is of primary interest because it predicts that the scintillation noise is translated in frequency to form upper and lower sidebands about the modulated signal. The bandwidth of each sideband is equal to the bandwidth of  $\phi_S(\omega)$ .



#### IV. EXPERIMENTAL PROCEDURE

##### A. BASIC EXPERIMENT

The basic experiment as originally conceived is shown in block diagram form in Figure 1. The laser and modulation equipment were located in a mobile facility positioned at a convenient shore location and the optical receiver and data recorder were located on the Acania.

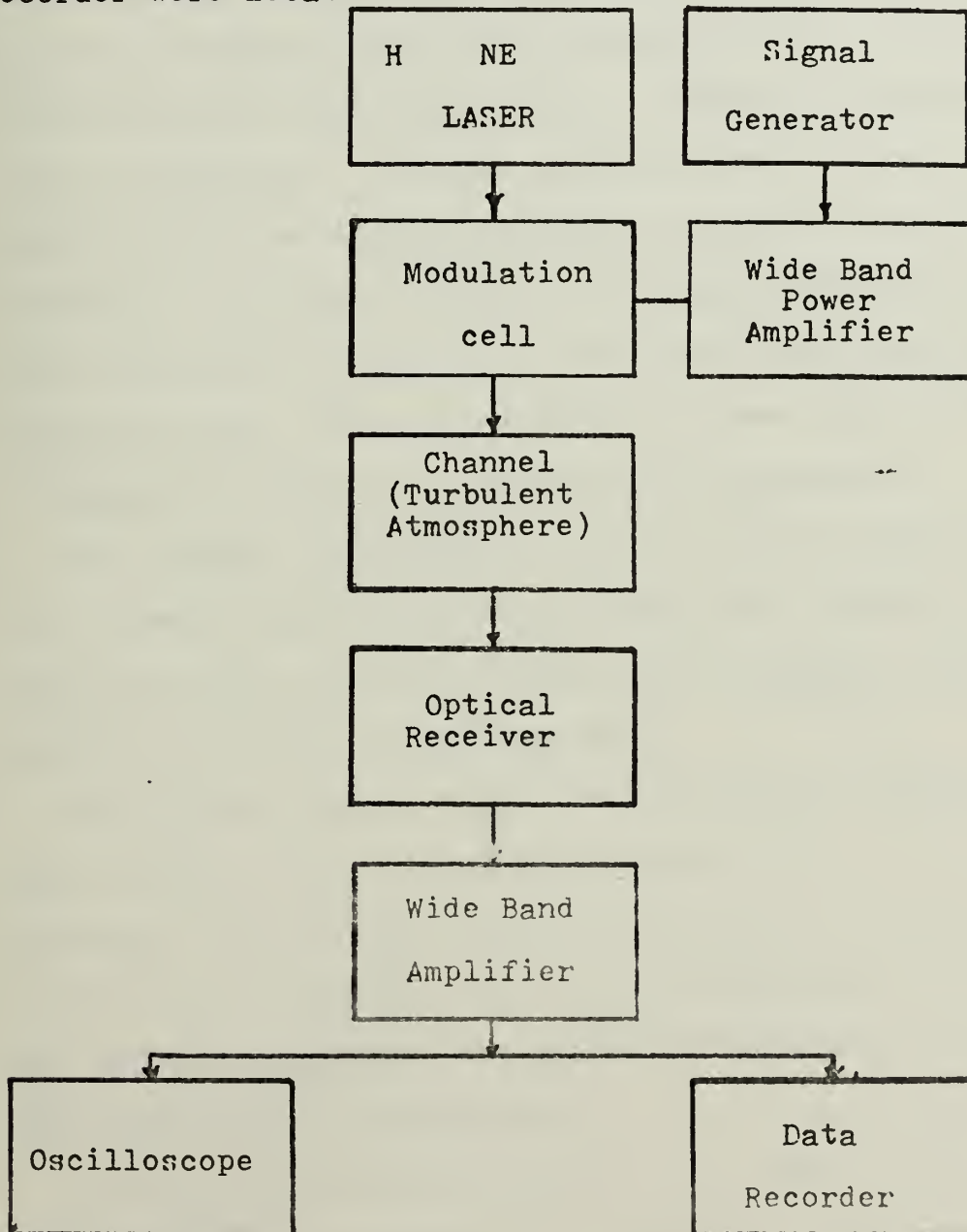


Fig. 1 Basic Experiment Block Diagram



The laser was a JODON model HN-15 Helium<sub>2</sub> neon laser operating at the 0.6328 $\mu$  wavelength line of He-Ne with a rated power output of 15 mW. It was mounted on a large steerable telescope which was used in the larger project.

The modulation of the laser beam at frequencies of 10 Hz to 10 kHz was accomplished initially by a handmade acoustoptic modulator designed and built by Rankin, which consisted of a distilled water cell acoustically excited by a gold-plated quartz transducer. A signal generator and wideband power amplifier fed the desired modulation signal to the quartz transducer. The acoustoptic modulator was capable of splitting about 25 percent of the laser beam power into the modulated beam. This relatively low power output necessitated a subsequent shift to an electro-optic modulator.

The channel consisted of a nominal path length of 1.5 to 2 km through normally turbulent atmosphere between the shore location of the mobile facility and the Acania, which was normally at anchor in Monterey Bay.

The optical receiver for the experiment consisted of a MERET hybrid detector/amplifier mounted with a 1.5 inch diameter, 4 inch focal length lens mounted on a stabilized platform on the Acania. The detector/amplifier output was then further amplified by a HEWLET-PACKARD Model 450A wide-band amplifier with 40 dB gain.

The signal was then recorded on an AMPEX SP-300 instrumentation recorder at 15 inches per second on one quarter inch high output/low noise magnetic tape. Signal



monitoring was accomplished on a general purpose oscilloscope.

## B. REVISED EXPERIMENT

Detector sensitivity inadequacies led to compatibility problems with Dr. Crittenden's project, hence an independent data collection effort was required. The requirements of the larger project resulted in the need to diverge the laser beam (shore to ship link) in order to allow for automatic tracking with the stabilized shipboard system in the presence of ship's motion. The divergence of the laser beam resulted in a laser beam power density at the ship considerably below the threshold required for detection with the MERET detector/amplifier.

Thus, a revised experiment was devised which operated over a shorter path length. Figure 2 shows the revised experiment in block diagram form. This experiment was conducted on the rooftop of a building of the Naval Postgraduate School and used a mirror to achieve a total path length of about 300 meters. The electro-optic modulator was used and the other equipment remained the same.

Preliminary data and calibration trials indicated that the signal distortion and noise added by the tape recorder were excessive, hence a further modification of the experiment was performed with the tape recorder completely removed and the amplified output signal of the detector/amplifier fed directly to a spectrum analyzer. Figure 3 shows the final form of the experiment.





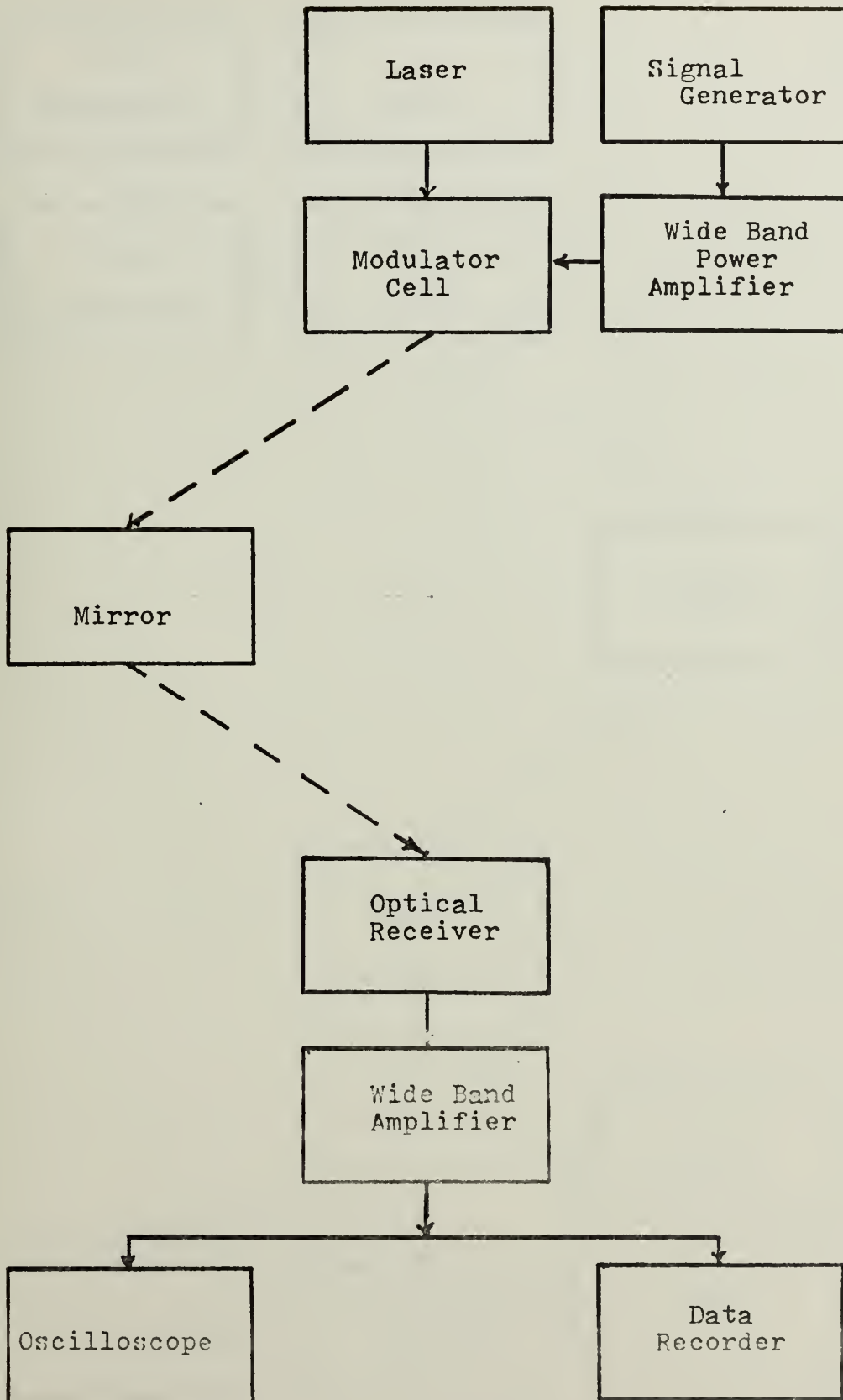


Fig. 2 Revised Experiment Block Diagram



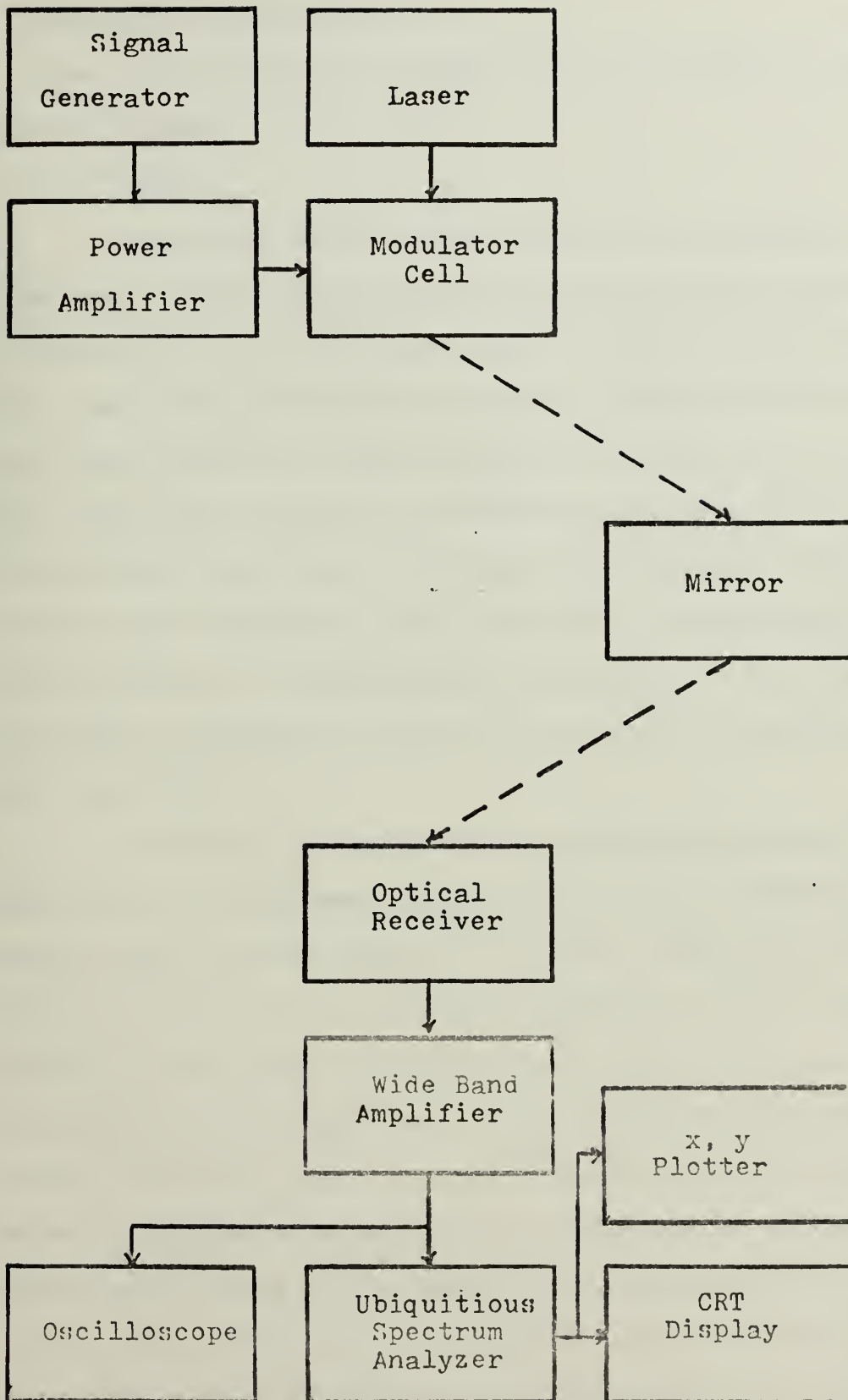


Fig 3. Final Experiment Block Diagram



### C. EQUIPMENT DESCRIPTION

The specific equipment ~~used in the~~ experiment of Figure 2 was as follows:

#### 1. LASER.

Two lasers were used in the final experiment. The first was a JODON Model HN-15 Helium-Neon laser<sup>\*</sup> operating at a wavelength of  $0.6328\mu$  with a rated power output of 15 mW. This laser had end mirrors completely separate from the laser tube which permitted easy adjustment for maximum power output, but often required re-adjustment as the unit was quite susceptible to movement and vibration. Further, the power supply high voltage for this unit had a strong ripple in it which resulted in a substantial modulation of the laser at the ripple frequency of 120 Hz as well as at harmonics of that frequency.

The second laser used was a METROLOGIC Model ML-669 laser, also helium-neon and operated at the  $0.6328\mu$  wavelength, with a power output of 0.8 mW. This unit had internal circuitry that permitted modulation of the discharge current in the laser tube, thus permitting direct intensity modulation of the laser beam without any external modulator. However, the lower limit of the bandwidth specified for this internal modulation capability was only 300 Hz which was considerably above desired modulation frequencies of 10, 20, 50, 100, and 200 Hz. In spite of this bandwidth limitation, sufficient modulation depth was possible at these frequencies to permit detection and de-modulation by the





optical receiver. This unit also exhibited high voltage ripple, which appeared as intensity modulation at the ripple frequency and several harmonics.

## 2. MODULATOR

Modulation of the JODON laser was accomplished with a COHERENT ASSOCIATES Model 3003 Modulation System, consisting of a transverse field electro-optic modulator driven by a solid state direct-coupled broadband power amplifier.

The modulator driver input was a one volt signal at the desired frequency from a WAVTEC Model 142 Signal Generator. This signal is amplified and combined with a variable bias voltage and applied to the electro-optic crystal. Driver voltage is sufficient to modulate the laser beam 100 percent. The variable bias voltage allows precise adjustment of the modulator cell operating point.

The driver output applied to the modulator cell produces a change in the index of refraction of the electro-optic crystal through which the laser beam travels. This effect is converted to intensity modulation by subsequent passage through a polarizer window.

The system bandwidth is D.C. to 3 MHz, with rise and fall times of 140 nanoseconds for all drive levels. Optical transmission through the modulator cell is greater than 80 percent.

For comparison purposes, the METROLOGIC laser was also modulated with this electro-optic system.

The METROLOGIC laser was also modulated directly,



utilizing its internal modulator driver to modulate the discharge current in the laser tube, thus directly modulating the laser beam output. This system modulates about 15 percent with a bandwidth of 300 Hz to 500 kHz. In spite of the 300 Hz lower limit, it was found that sufficient modulation was achieved at frequencies down to and including 10 Hz to allow retrieval of the modulating signal with the MERET detector/amplifier.

### 3. OPTICAL RECEIVER SYSTEM

The heart of the optical receiver consisted of an integrated circuit photo-diode detector with an amplifier on the same chip manufactured by MERET INC. (Model FDA 425). This detector amplifier was mounted at the focal point of a lens and filter system. The lens was an uncorrected, 4 inch focal length, 1.5 inch diameter type. The optical filter had a transmissivity of 0.85 at 6328 angstroms and a bandwidth of 30 Angstroms. The lens and filter were mounted in an aluminum cylindrical housing with the detector/amplifier suitably mounted at the rear of the assembly.

This receiver assembly had an effective collection aperture of about  $11 \text{ cm}^2$ . The purpose of the optical filter was to reduce background light contributions, since the photo-diode had a spectral range that included the visible spectrum, specifically from  $0.36\mu$  to  $1.15\mu$ . The responsivity curve for the FDA 425 device is shown in Figure 4. The bandwidth specifications for the device were D.C. to 10 mHz with a rise time of less than 40 nanoseconds, which was



very compatible with the bandwidth of the electro-optic modulator system.

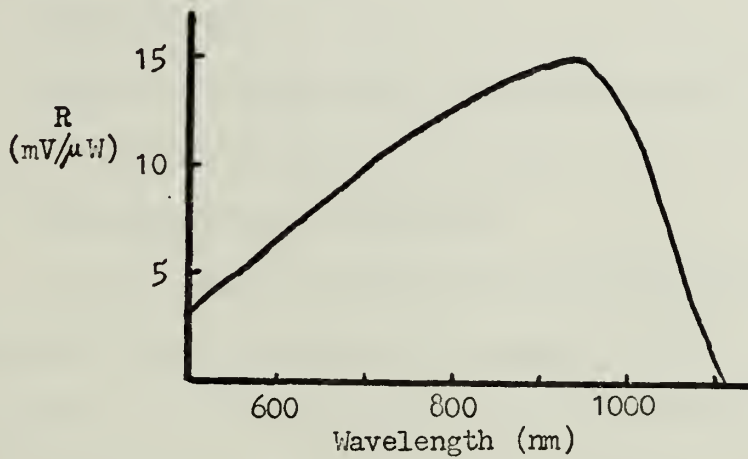


Figure 4. Responsivity of MERET FDA 425 Detector/Amp

The photo-diode portion of the device had an active area of  $4.5 \text{ mm}^2$  and a rated Noise Equivalent Power  $/(\text{Hz})^{\frac{1}{2}} \text{ W}$   $(\text{Hz})^{\frac{1}{2}}$  at  $0.905 \mu$ . This led to the belief that this device possessed sufficient sensitivity to permit its use with an expected power density of a few nqnowatts per square centimeter which was the power level achieved at the Acania. This sensitivity was not realized and a revised experiment had to be devised to gather the data. The sensitivity question is covered in more detail in section D of this chapter.

#### 4. WIDEBAND AMPLIFIER

The wideband amplifier used in the experiment was a HEWLETT-PACKARD Model 450A unit with selectable gain of either 20 or 40 dB. Laboratory test of this unit showed essentially flat response from 5 Hz to over 100 kHz at both





gain settings. The rms noise voltage was specified as 40 $\mu$ V, which became significant when attempting to work at very low power densities.

#### 5. OSCILLOSCOPE

The oscilloscope used to monitor the detector output was a TEKTRONICS Model 422 unit.

#### 6. INSTRUMENTATION RECORDER

In the initial experiment the amplified output of the detector was recorded on an AMPEX SP-300 Ibstrynebta-tion Recorder at 15 ips with direct recording. The frequency response specifications for this recorder at 15 ips were 20 Hz to 40 kHz. Roll-off at the lower frequencies plus an excessive amount of tape recorder related noise led to the final modification of the experiment which eliminated the recorder all together. Section E of this chapter deals in more detail with the tape recorder difficulties encountered.

#### D. OPTICAL RECEIVER SENSITIVITY

As mentioned earlier, the achieved sensitivity of the detector/amplifier failed to meet the needs of the original experiment and resulted in a revision to it. After the lack of sufficient sensitivity was realized, a series of laboratory tests were conducted to determine more exactly the actual sensitivity of the detector in the form of minimum discernible power requirements.

The test consisted of using a combination of Neutral Density Filters with known filter factors to reduce the strength of a known power level laser beam until the





detected signal became lost in the system noise. Figure 5 shows the test in block diagram form.

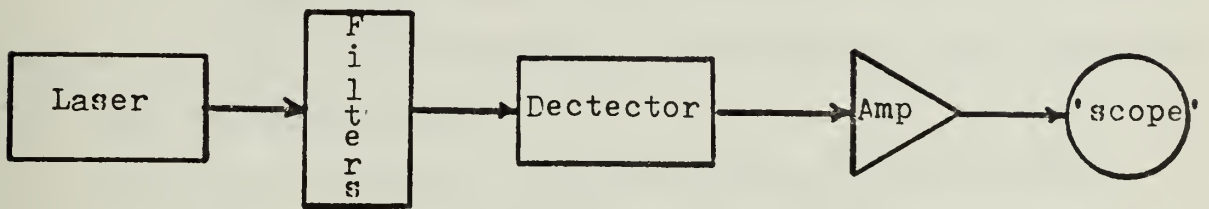


Fig. 5 Sensitivity test block diagram

The METROLOGIC laser was used and its output measured with an optical power meter at 0.83 mW. Several MERET FDA 425 devices were tested in the manner described above, both with and without the optical filter (6328 A) in the receiver assembly. In all cases, minimum power requirements were on the order of  $10^7$  watts in order to just barely discern the output of the detector/amplifier.

For comparison purposes, an identical test was performed on a UNITED DETECTOR TECHNOLOGY Model UDT-600 detector/amplifier. This IC is very similar to the MERET unit in all specifications, however, its implementation uses an external feedback resistor to control the sensitivity. This device was installed in the receiver lens/filter assembly and a feedback resistor selected for maximum sensitivity. The result was on the order of  $10^{-8}$  watts, only slightly better than the MERET unit performance.

An alternate test was conducted on the UDT device by using a wave analyzer to measure the output voltage with a very sharp filter to limit the noise bandwidth. With this



arrangement with a 6 Hz filter centered at the modulation frequency, the minimum discernible power was on the order of  $10^{-10}$  watts. This was a purely academic result, however, since the experiment required a considerably larger bandwidth.

#### E. TAPE RECORDER NOISE

As noted in section C of this chapter, difficulties with the AMPEX tape recorder in the form of excessive extraneous noise and low frequency rolloff resulted in the final modification of the experiment which analyzed the spectrum of the detector output directly with a Ubiquitous Spectrum Analyzer in real time, eliminating the use of the tape recorder altogether. Figure 6 shows the spectrum of the tape recorder output with the recorder idling. Significant noise line spectra appear at 20, 60, and 180 Hz. Figure 7 shows the spectrum of the recorder output for un-recorded, un-erased, factory fresh tape being played back at 15 inches per second. Additional noise line spectra appear at 40 and 50 Hz.



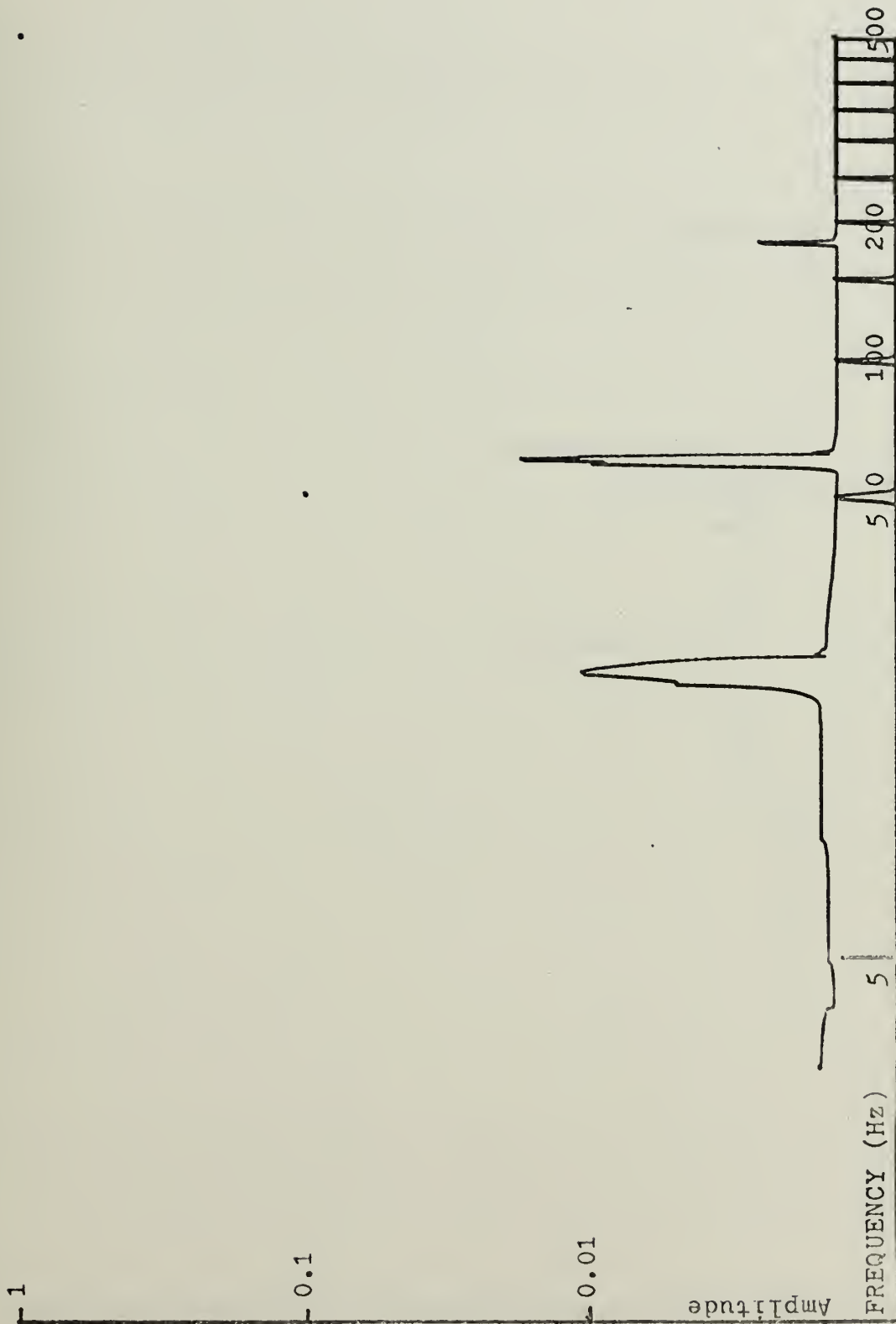


Fig. 6. Tape Recorder Output: Idling



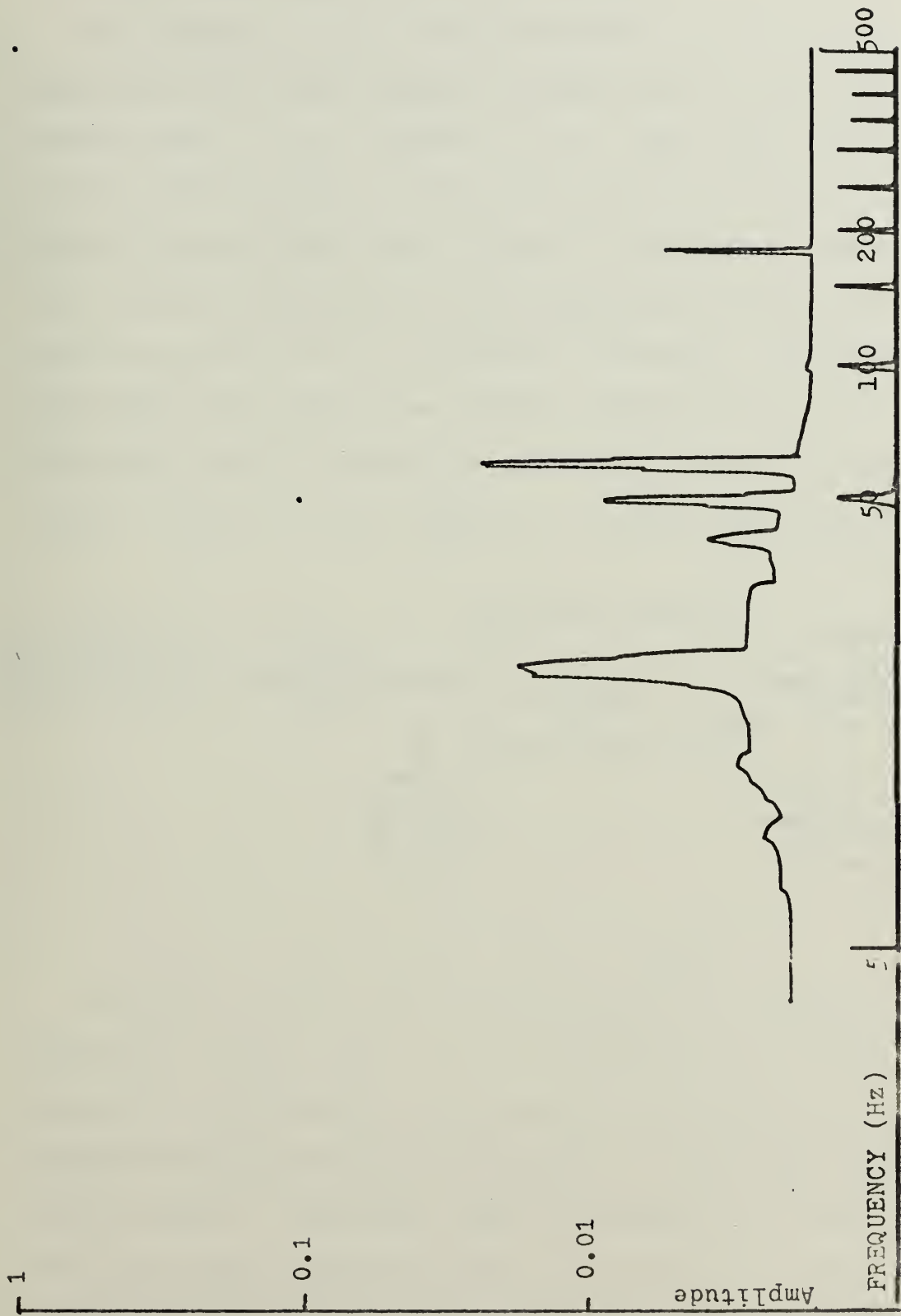


Fig. 7. Tape Recorder Output: Blank Tape





## V. DATA DESCRIPTION AND ANALYSIS

### A. DATA FORMAT AND REDUCTION TECHNIQUE

The output of the detector/amplifier was a voltage waveform in the time domain, the amplitude of which was proportional to the intensity of the laser beam incident on the active surface of the photo-diode portion of the hybrid detector/amplifier. Since the frequency spectrum of this waveform contains the low frequency scintillation spectrum as well as the modulated frequency, the data was processed with a spectrum analyzer and the resulting frequency domain information was plotted on an X,Y recorder. Figure 8 shows a block diagram of the data reduction method.

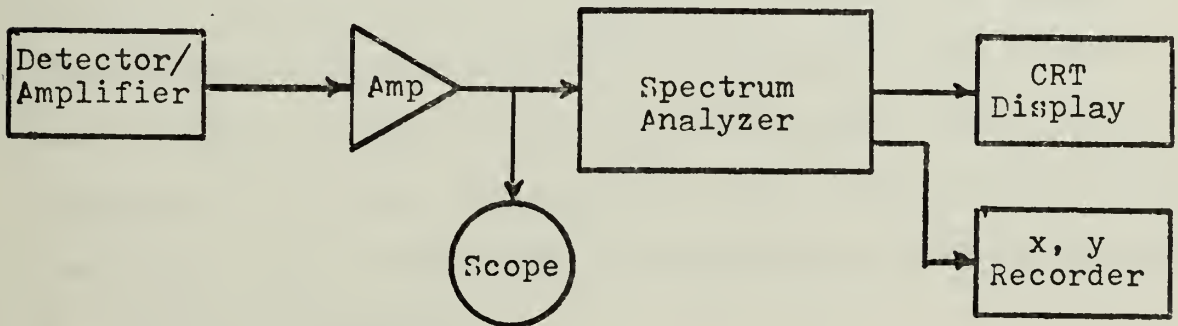


Fig. 8 Data Reduction Block Diagram

Spectrum analysis was accomplished with a Ubiquitous Spectrum analyzer (Model UA-500) manufactured by FEDERAL SCIENTIFIC CORPORATION. This analyzer performs real time analysis with an effective resolution of 650 lines (Horizontal scale). The input signal is sampled at a rate three times the upper cutoff frequency (Selectable as "ANALYSIS RANGE"). This rate is 1.5 times the Nyquist rate which



reduces aliasing errors to a negligible level. The samples are entered in parallel binary form into a recirculating memory; that is, memory output is fed back to the memory input, sequenced with respect to newly obtained samples so that the memory contains all samples in the order in which they arrive. The recirculation rate of the memory is much faster than the sampling frequency, hence the result is a speeded up replica of the input signal that retains all of the original frequency information (multiplied by a constant). This sped-up signal is then Fourier analyzed, using a step-heterodyning technique. The resulting spectra can be displayed on a CRT display unit. A spectra averaging option on this unit may be used to average up to  $1024$  of these instantaneous spectra and store the result in one of two memory banks. Either or both of these memory banks can be displayed on the CRT display and a slow read-out mode allows the memory bank contents to be transferred to an X,Y recorder.

## B. NOISE/INTERFERENCE

Figure 9 shows the experiment block diagram. Spectra were taken at point A, the output of the signal generator; point B, the input to the electro-optic modulator cell; and at point C, the output of the amplifier following the optical receiver. This method helped to identify the sources for the various noise line spectra that appeared in the spectra at point C.

Figure 10 is a log-log plot of the spectrum of the output of the Modulator Driver (Point B) when no signal is



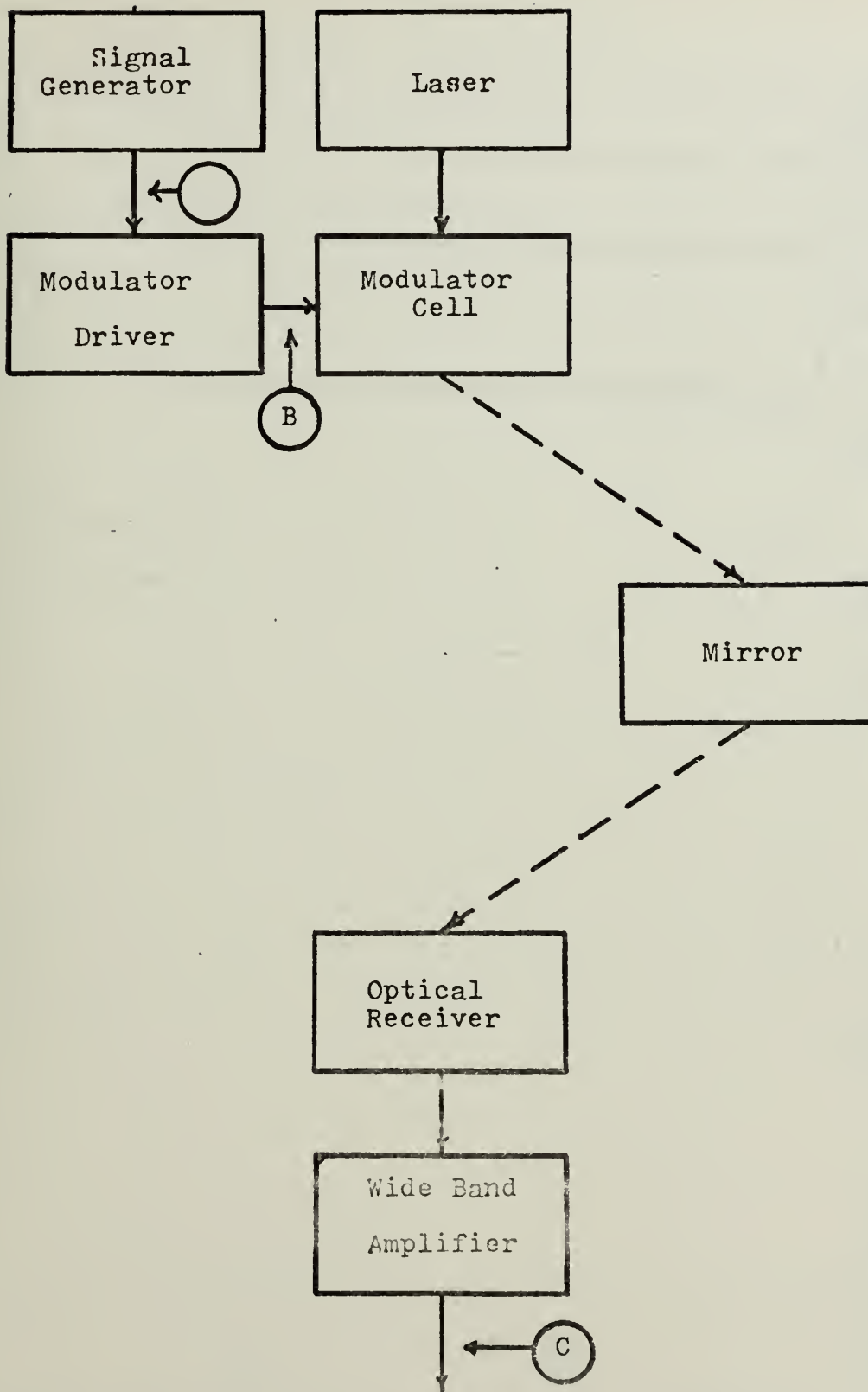


Fig. 9. Experiment Block Diagram Showing Data Points.



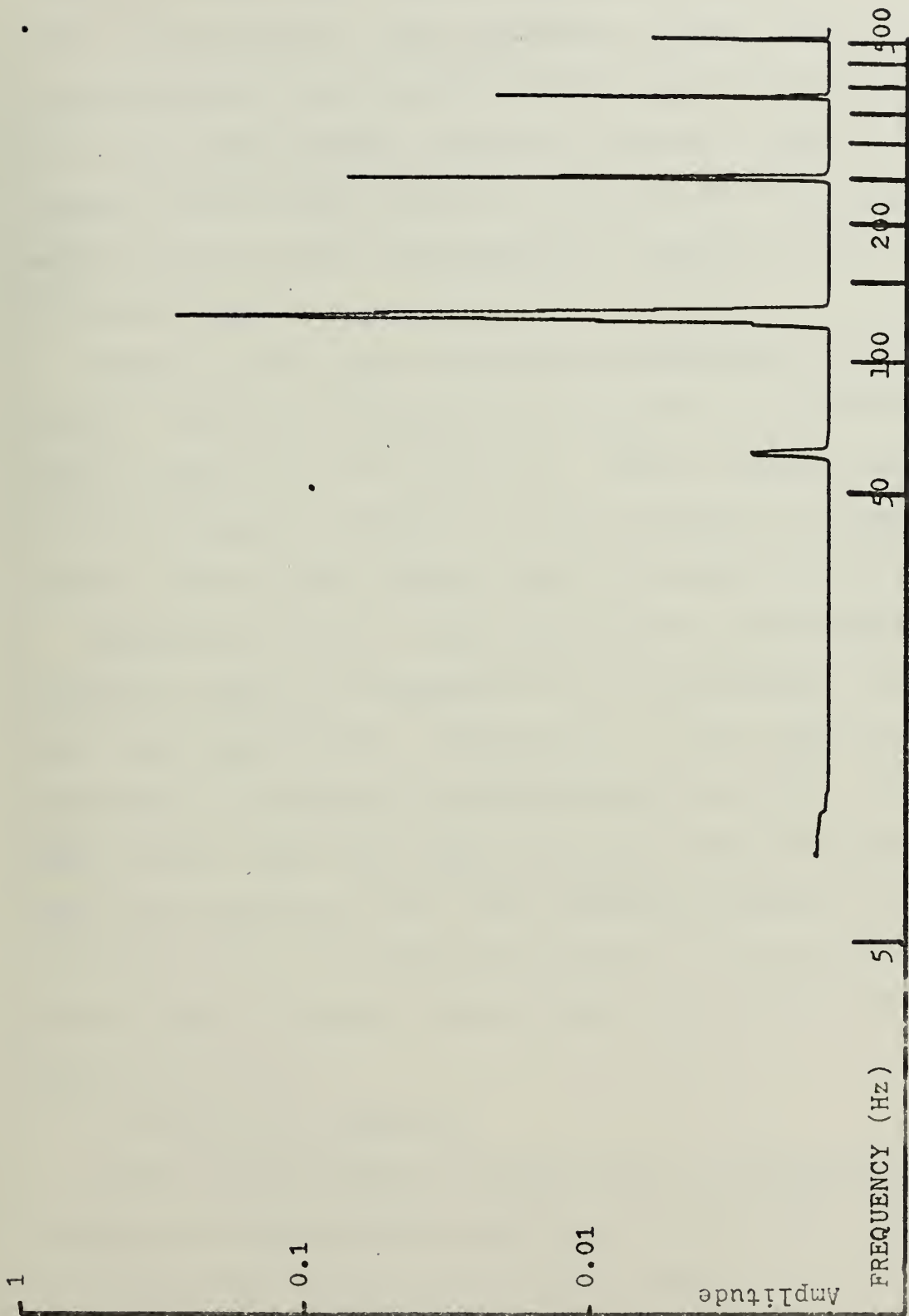


Fig. 10. Modulator Driver Output with no Input





applied to the input. Noise line spectra appear at 60, 120, 240, 360, and 480 Hz. The amplitude of these lines is exaggerated due to the reduction of the attenuation at the input of the spectrum analyzer, however, as will be seen in other figures, power supply ripple in the modulator driver does appear in the output, and therefore is applied to the input of the E/O cell.

Figure 11 is a plot of the signal generator output at 10 Hz. (Point A) and Figure 12 is a plot of the Modulator Driver output at 10 Hz (Point B). Notice that the harmonic at 20 Hz present in Figure 11 is also present in Figure 12, and the Driver power supply ripple at 120 Hz is added.

Figures 13, 15, 17, and 19 are plots of the signal generator output at frequencies of 50 Hz, 200 Hz, 1 kHz, and 5 kHz respectively. Figures 14, 16, 18, and 20 show the Modulator output at corresponding frequencies. Notice that in each case, the signal generator output includes a small line spectra at the first harmonic frequency which is carried over to the Modulator Driver output with the 120 Hz ripple frequency (plus harmonics) added by the Modulator Driver.

### C. SCINTILLATION SPECTRUM

Since scintillation is proportional to atmospheric turbulence, the scintillation spectrum should change over time to reflect the level of atmospheric turbulence. Therefore, a series of data was taken of the scintillation alone, that is, with an unmodulated laser beam, over a period of about



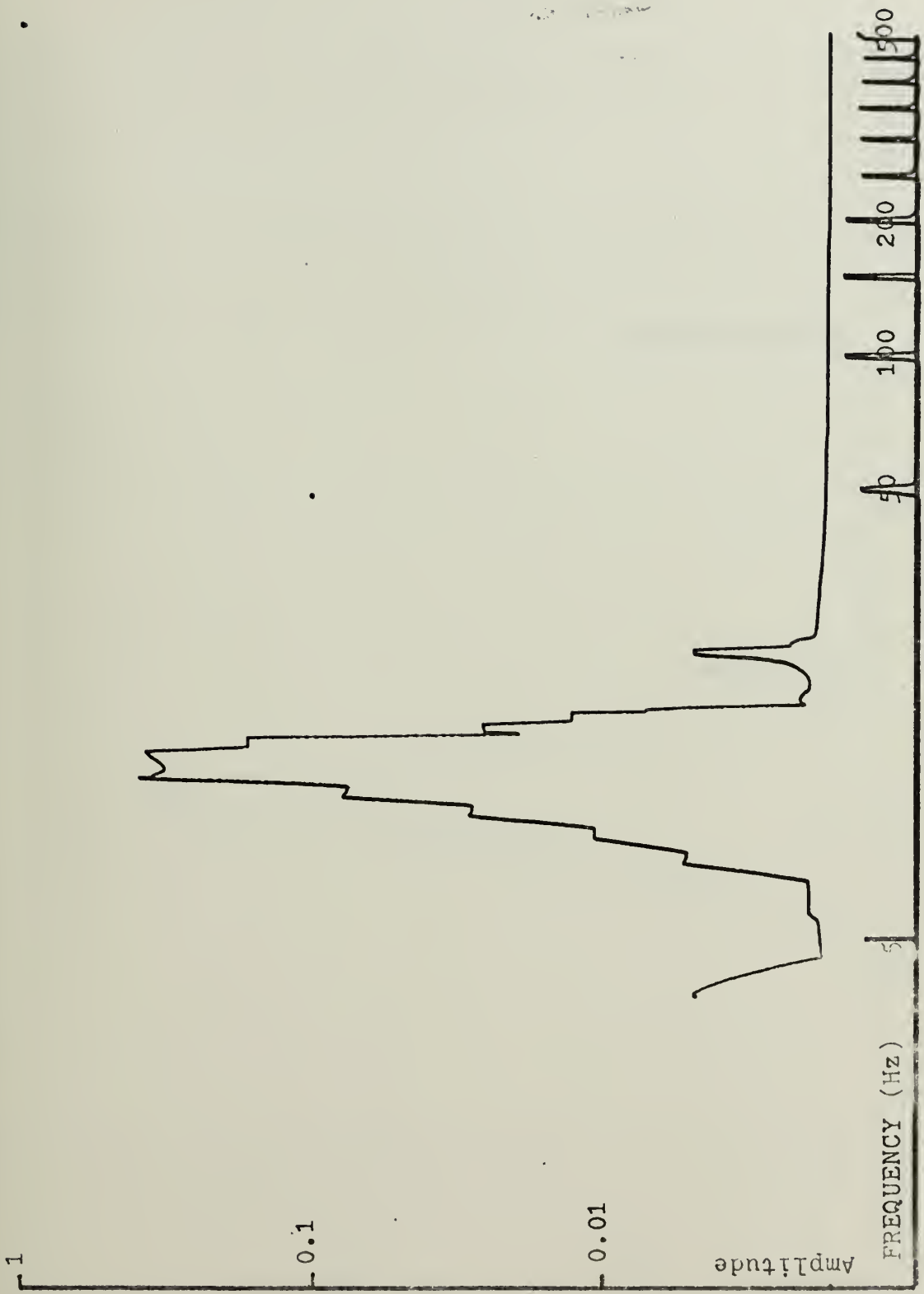


Fig. 11. Signal Generator Output: 10 Hz



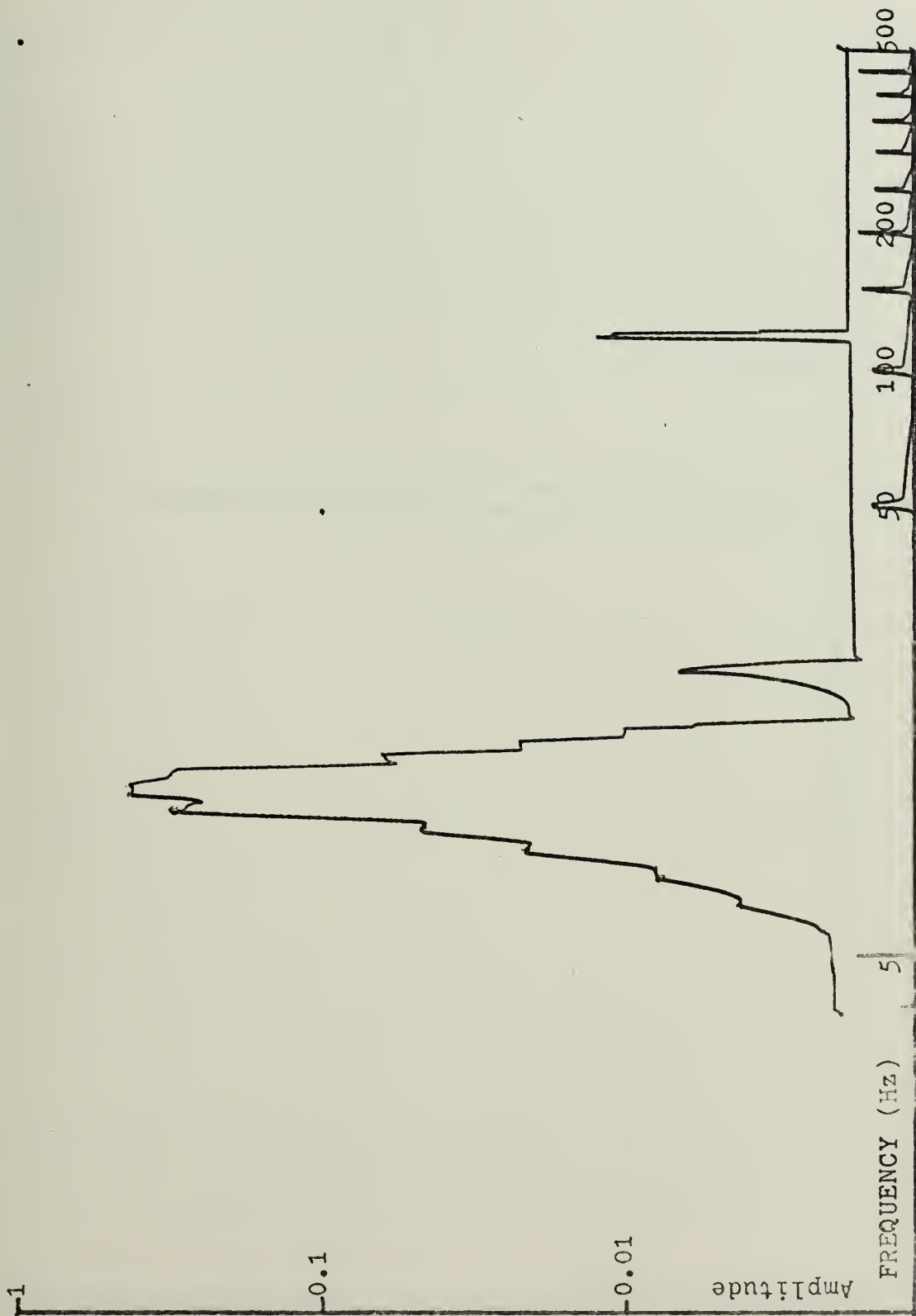


Fig. 12. Modulator Driver Output: 10 Hz



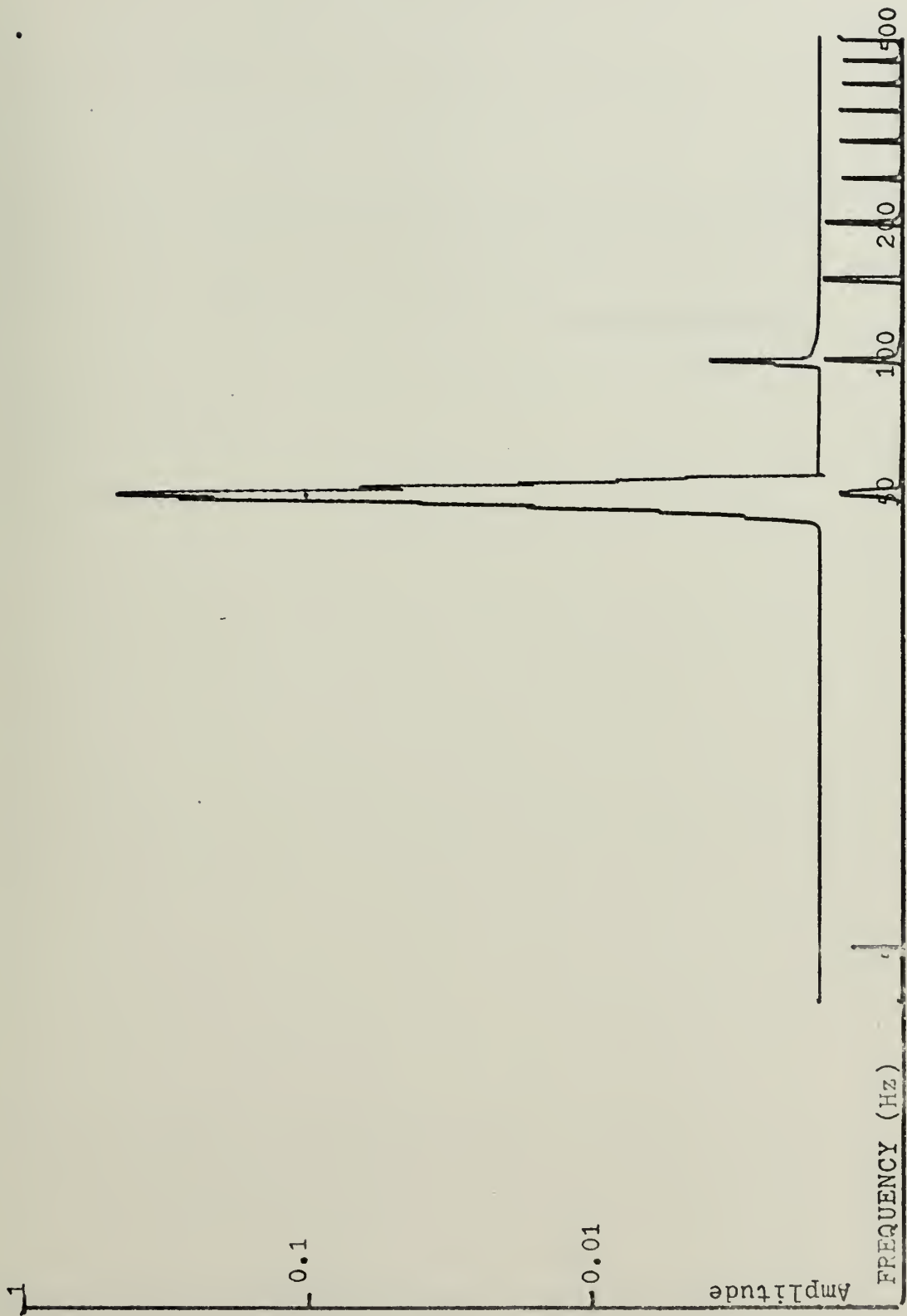


Fig. 13. Signal Generator Output: 50 Hz





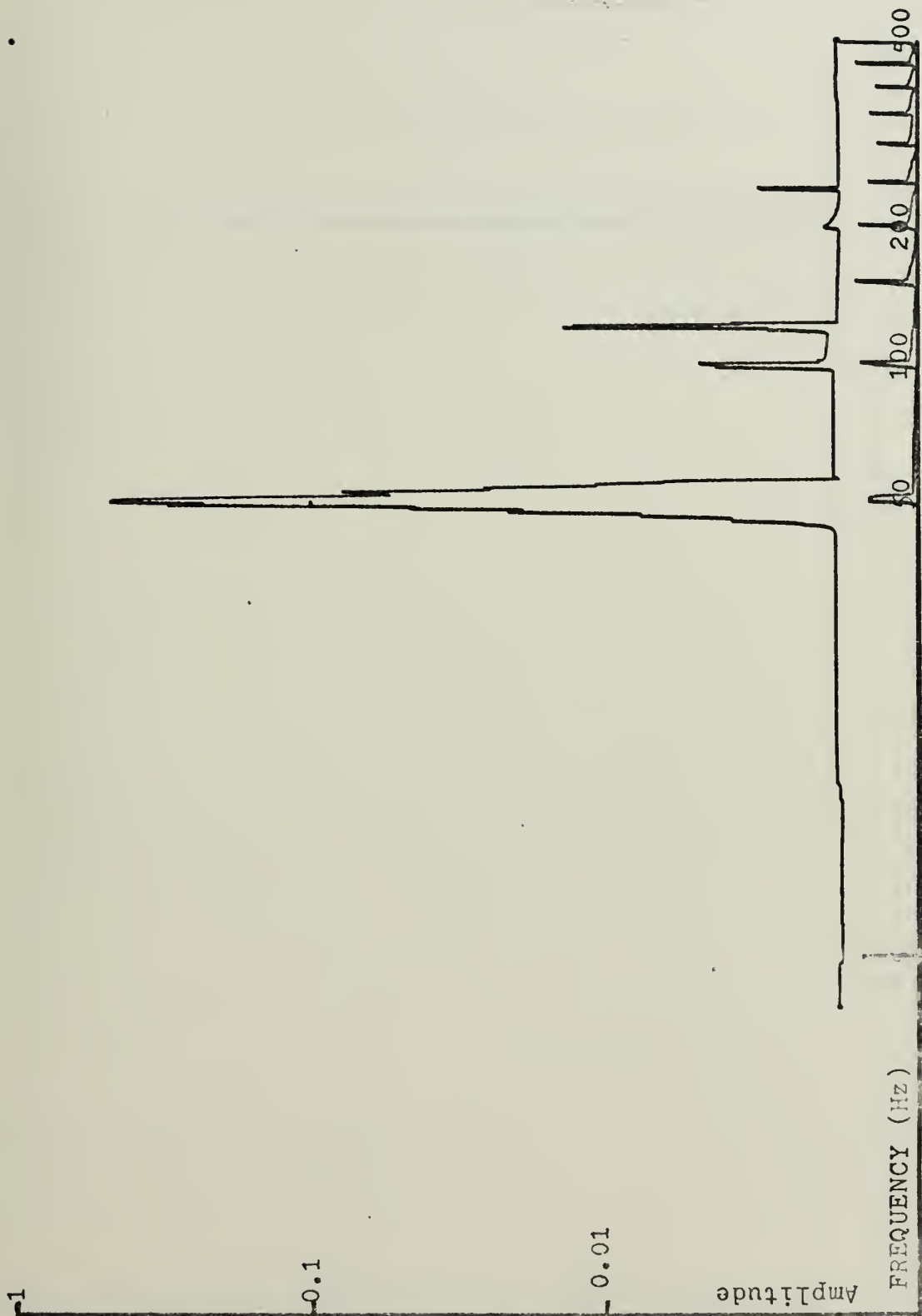


Fig. 14. Modulator Driver Output: 50 Hz



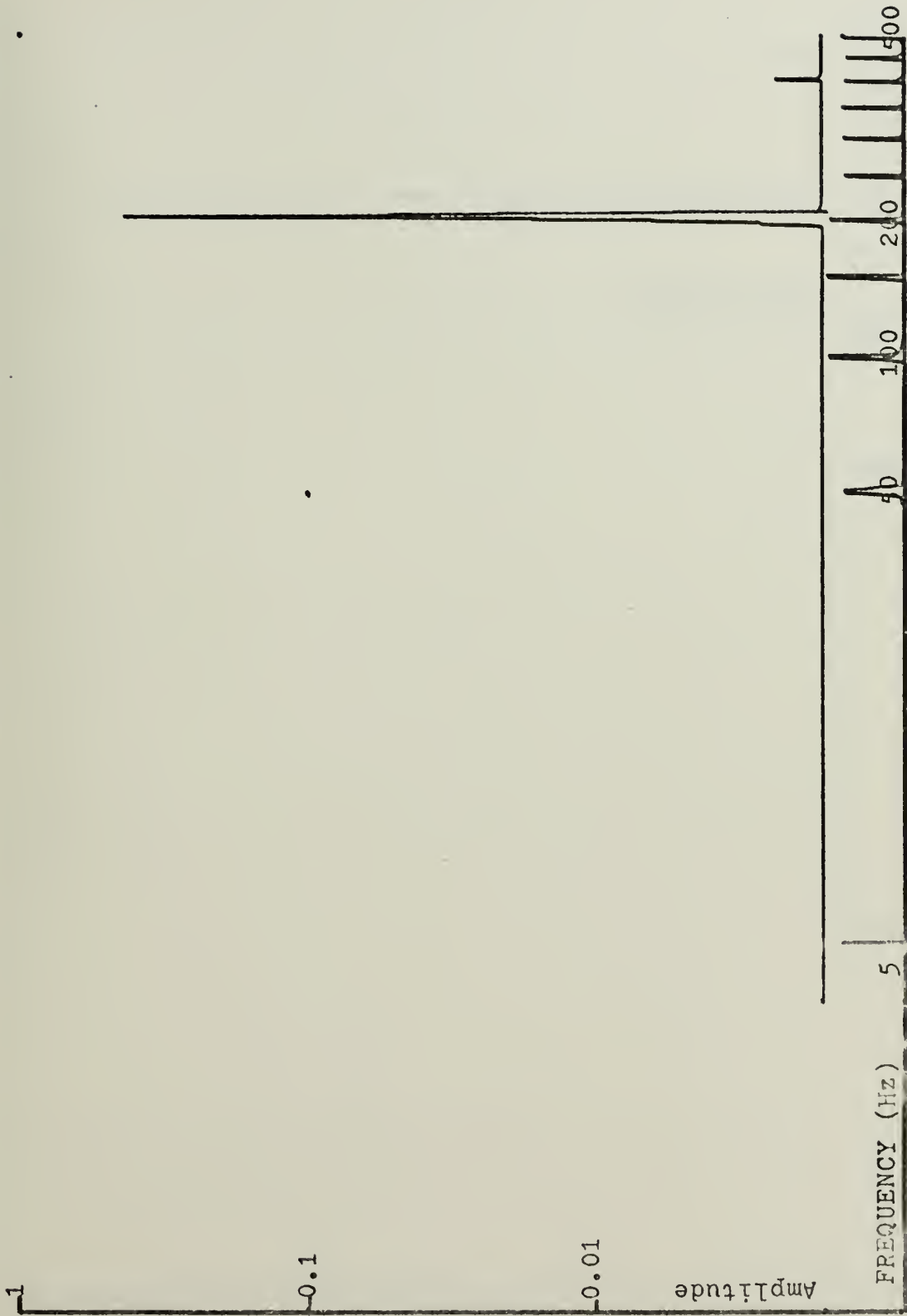


Fig. 15. Signal Generator Output: 200 Hz



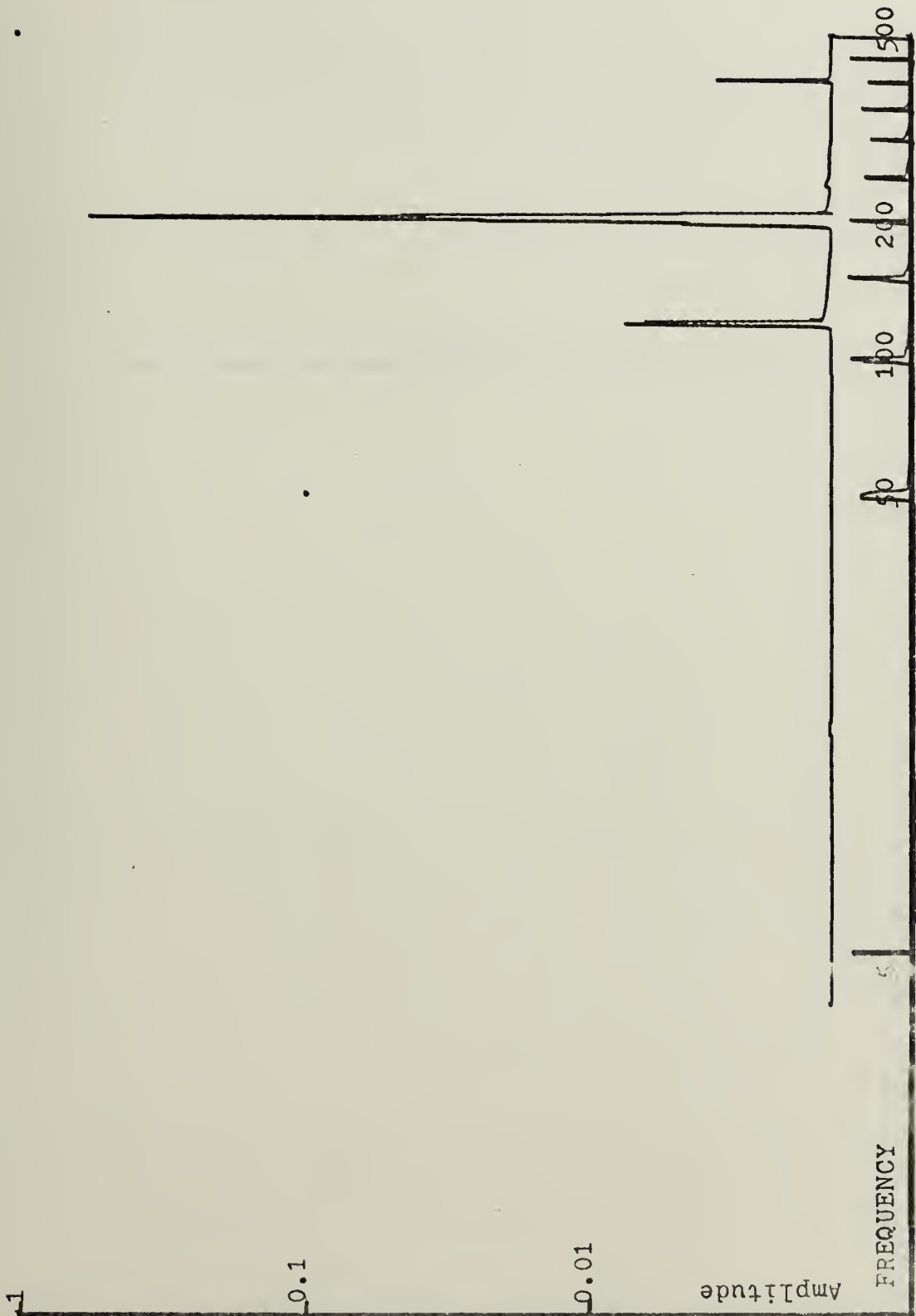


Fig. 16. Modulator Driver Output: 200 Hz



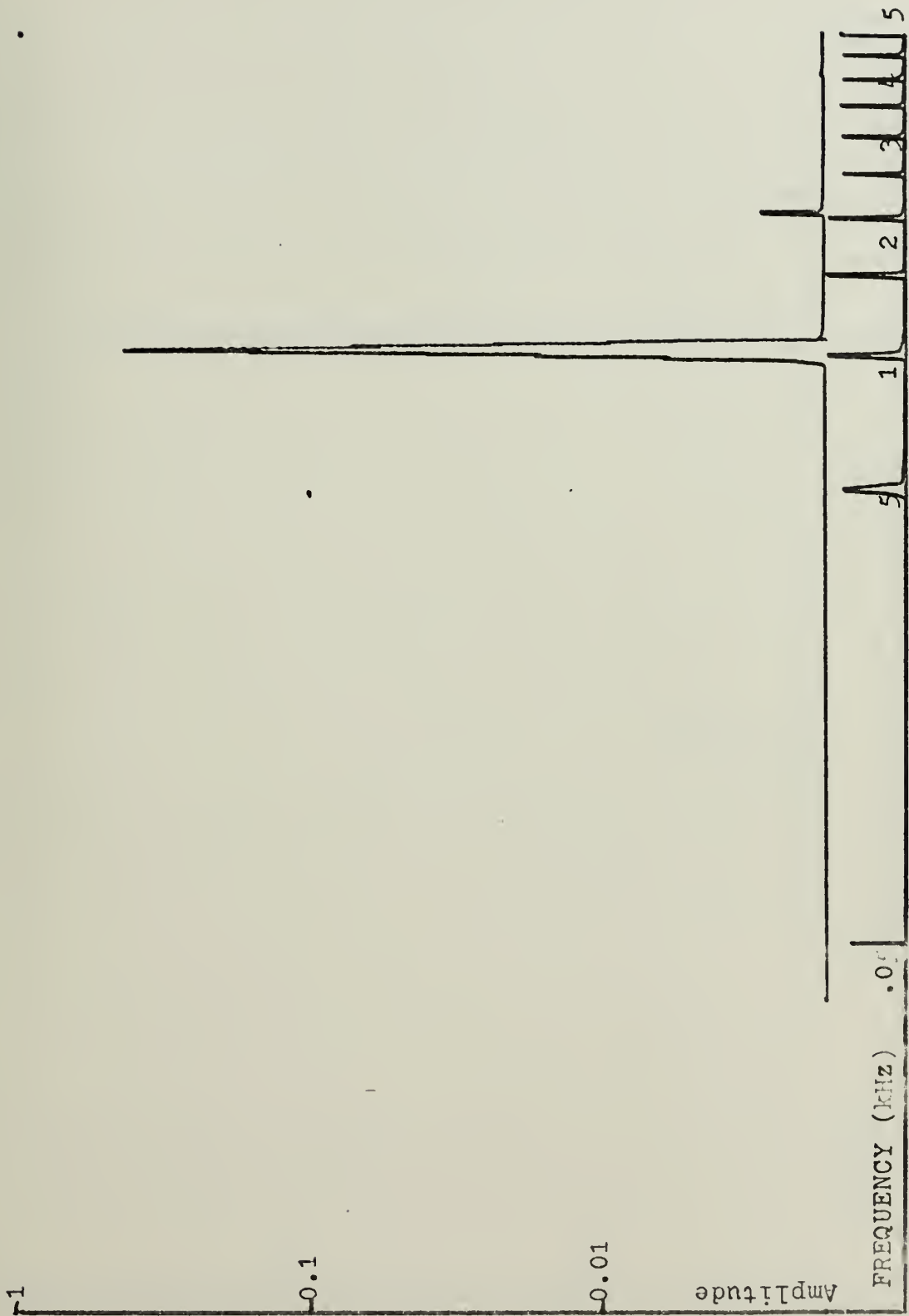


Fig. 17. Signal Generator Output: 1 kHz





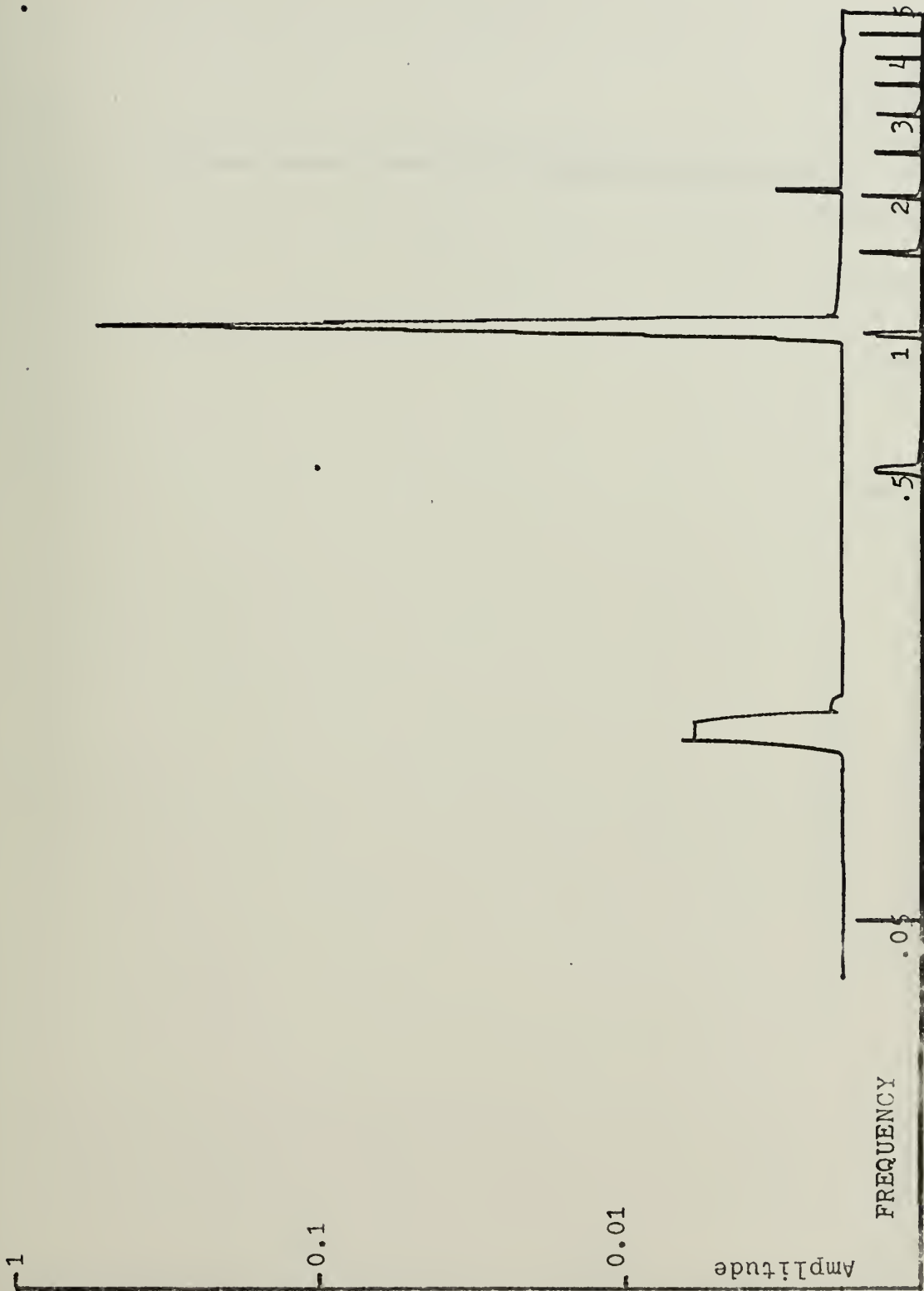


Fig. 18. Modulator Driver Output: 1 kHz



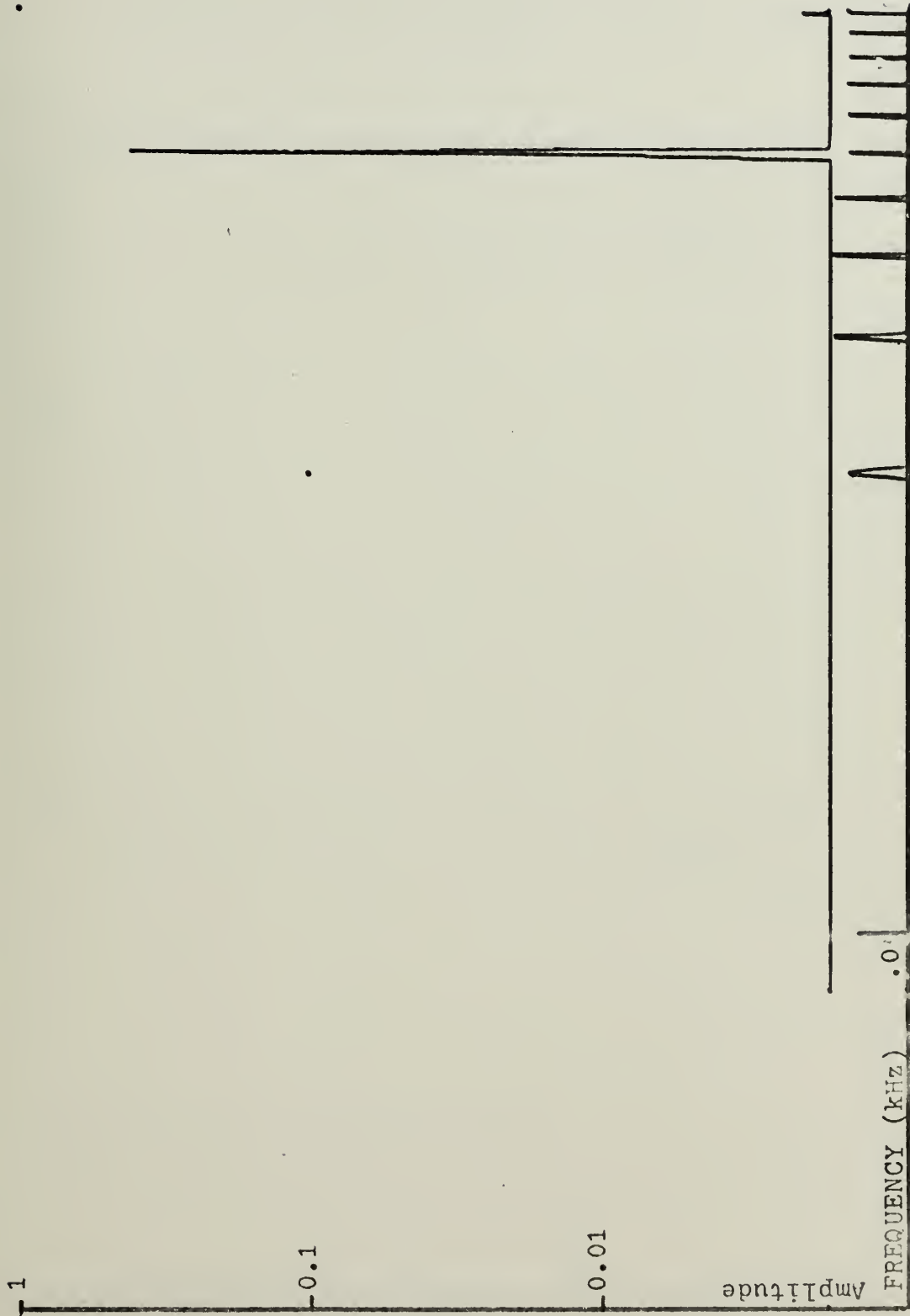


Fig. 19. Signal Generator Output: 5 kHz



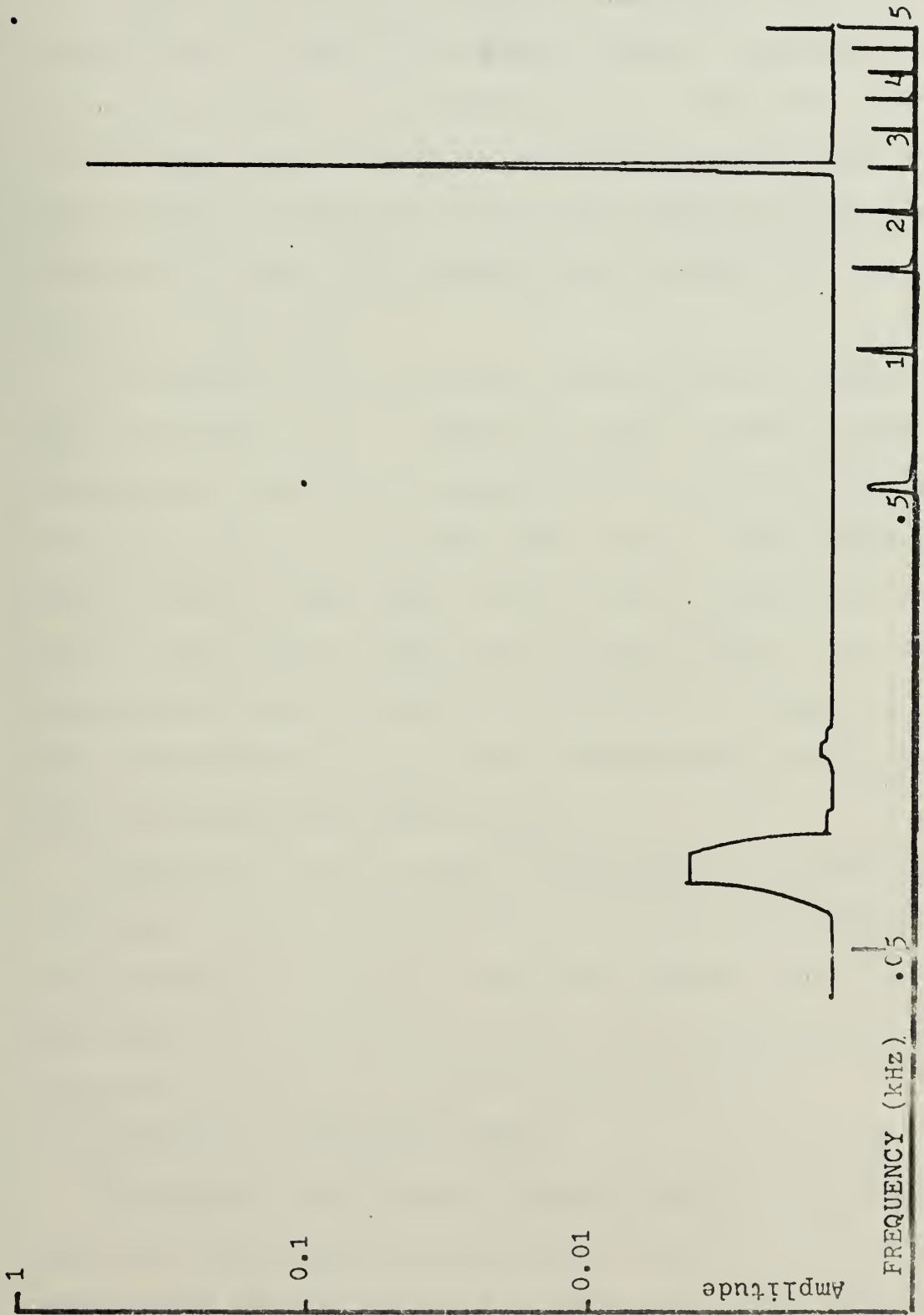


Fig. 20. Modulator Driver Output: 5 kHz



seven hours, at roughly one-half hour intervals. Figure 21 is a log-log plot of scintillation amplitude versus frequency taken at 0035, 12 November, 1974. The scintillation spectrum extends out to almost 300 Hz. The noise line spectra at 120, 180, 240, and 360 Hz are high voltage ripple in the laser itself. Figure 22 is the same spectrum taken about 40 minutes later. The spectrum was extended out to about 350 Hz at that time.

The scintillation spectrum stayed about the same for the next two hours or so. Figure 23, taken at 0340, shows that the spectrum had then increased out to about 400 Hz. About 30 minutes later a noticeable wind came up, and Figure 24, taken at 0417, shows that the spectrum was extended to over 900 Hz. By 0500 the wind had died down somewhat and the spectrum was reduced slightly, as shown in Figure 25. By 0547, when Figure 26 was taken, the spectrum had dropped back to a little more than 250 Hz.

Figures 27, 28, 29, and 30 were taken at fifteen minute intervals between 0615 and 0700, covering the transition from darkness to sun-up. The plots show that the scintillation spectrum changed very little over this period, possibly increasing slightly from 300 to about 400 Hz.

#### D. SPECTRUM OF MODULATED LASER

To examine the effect of scintillation on an intensity modulated laser beam the METROLOGIC laser was modulated at frequencies of 10, 20, 50, 100, 200, 500, 1000, 2000, 5000, and 10000 Hz with the electro-optic modulator and with its







Fig. 21. Scintillation Spectrum : 0035



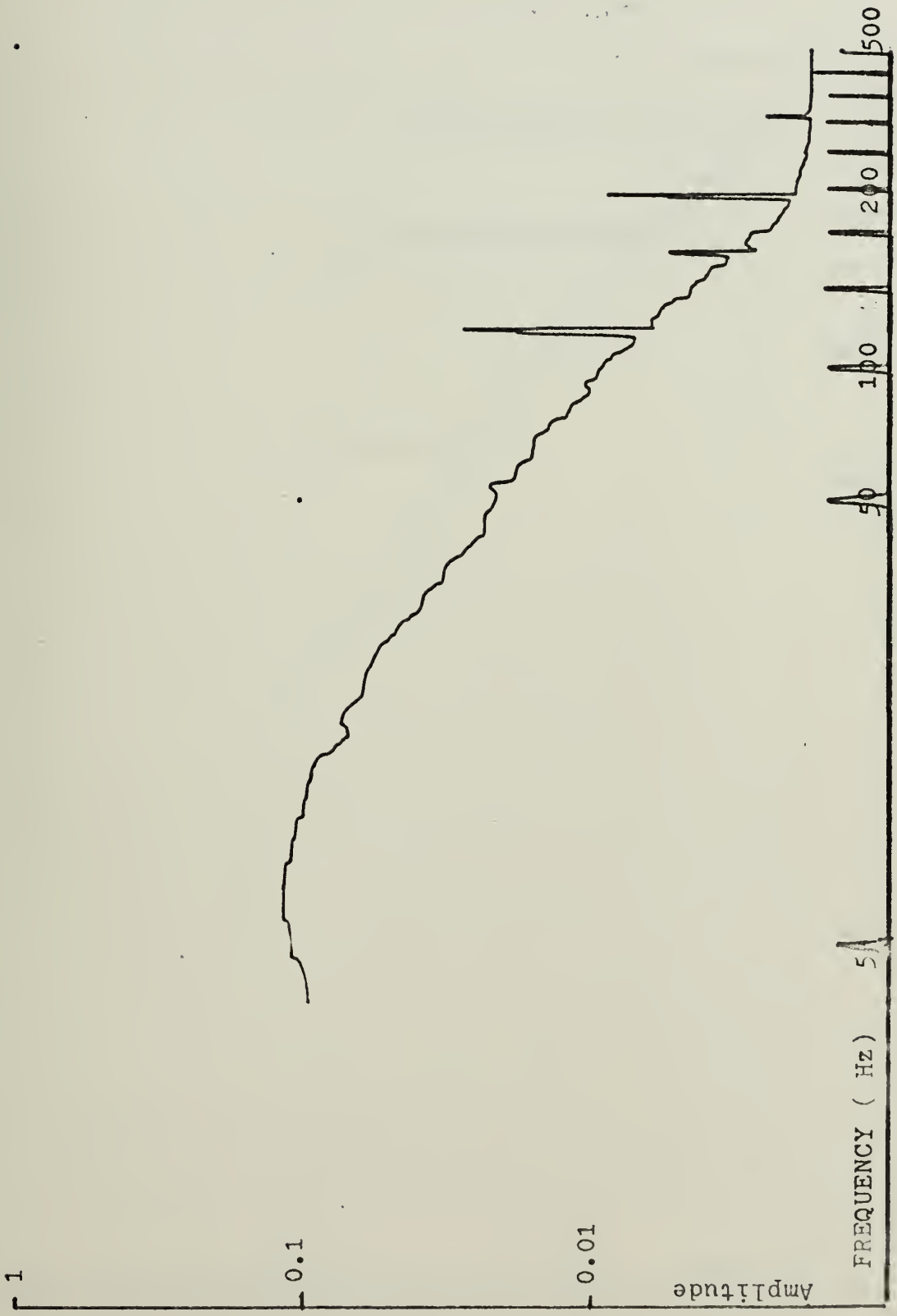


Fig. 22. Scintillation Spectrum: 0115



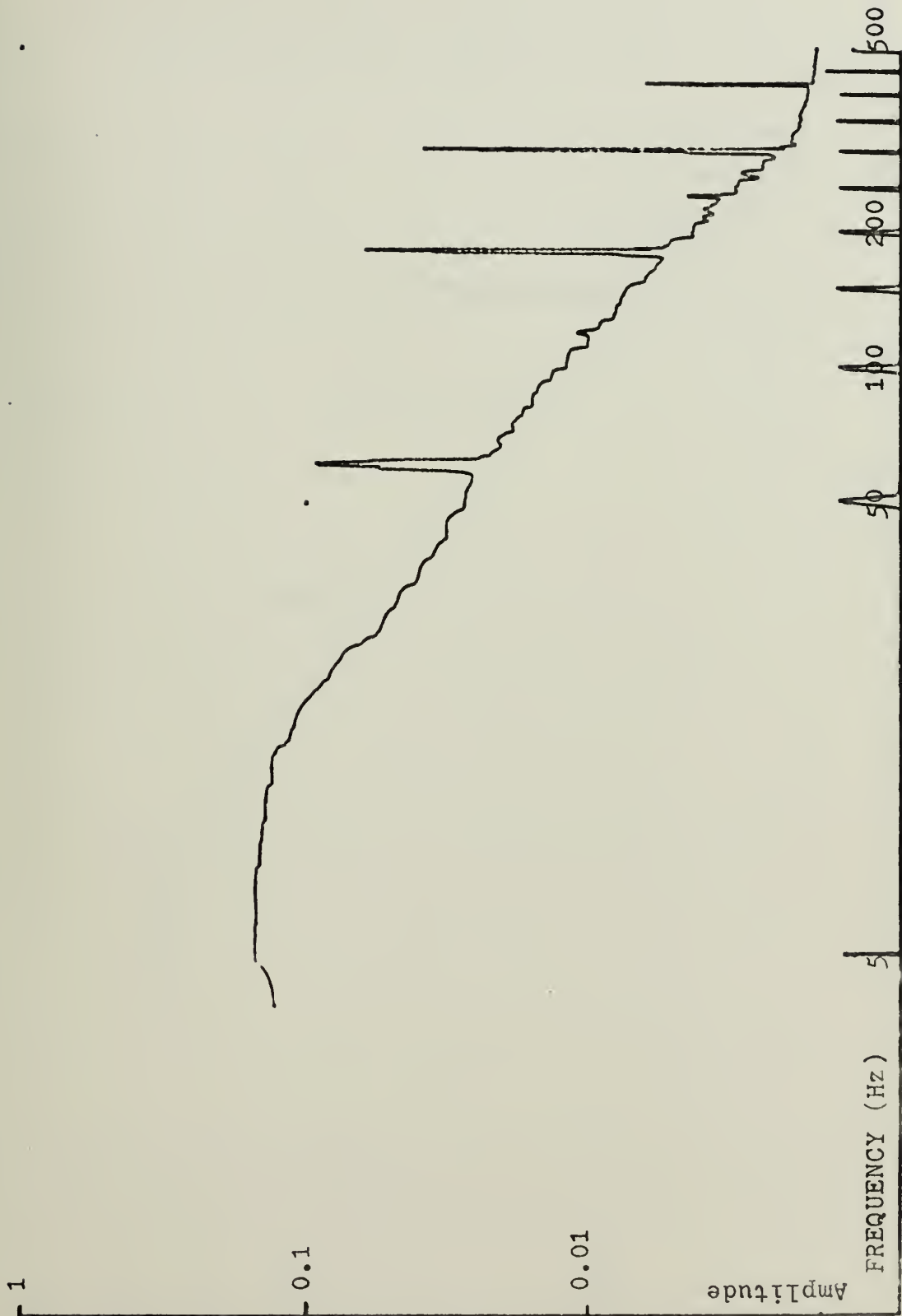


Fig. 23. Scintillation Spectrum: 0340





Fig. 24. Scintillation spectrum: 0417







Fig. 25. Scintillation Spectrum: 0500



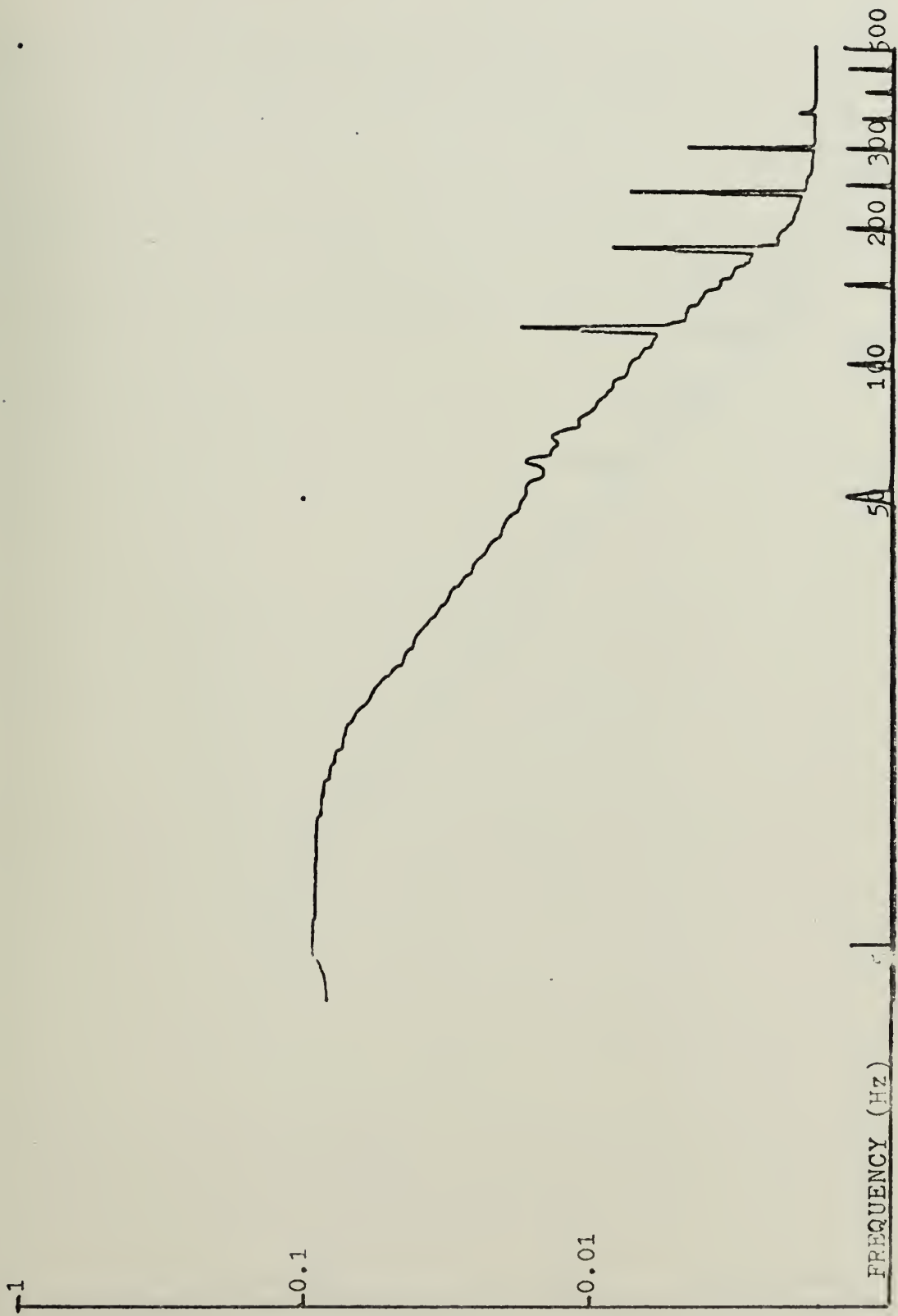


Fig. 26. Scintillation Spectrum: 0547



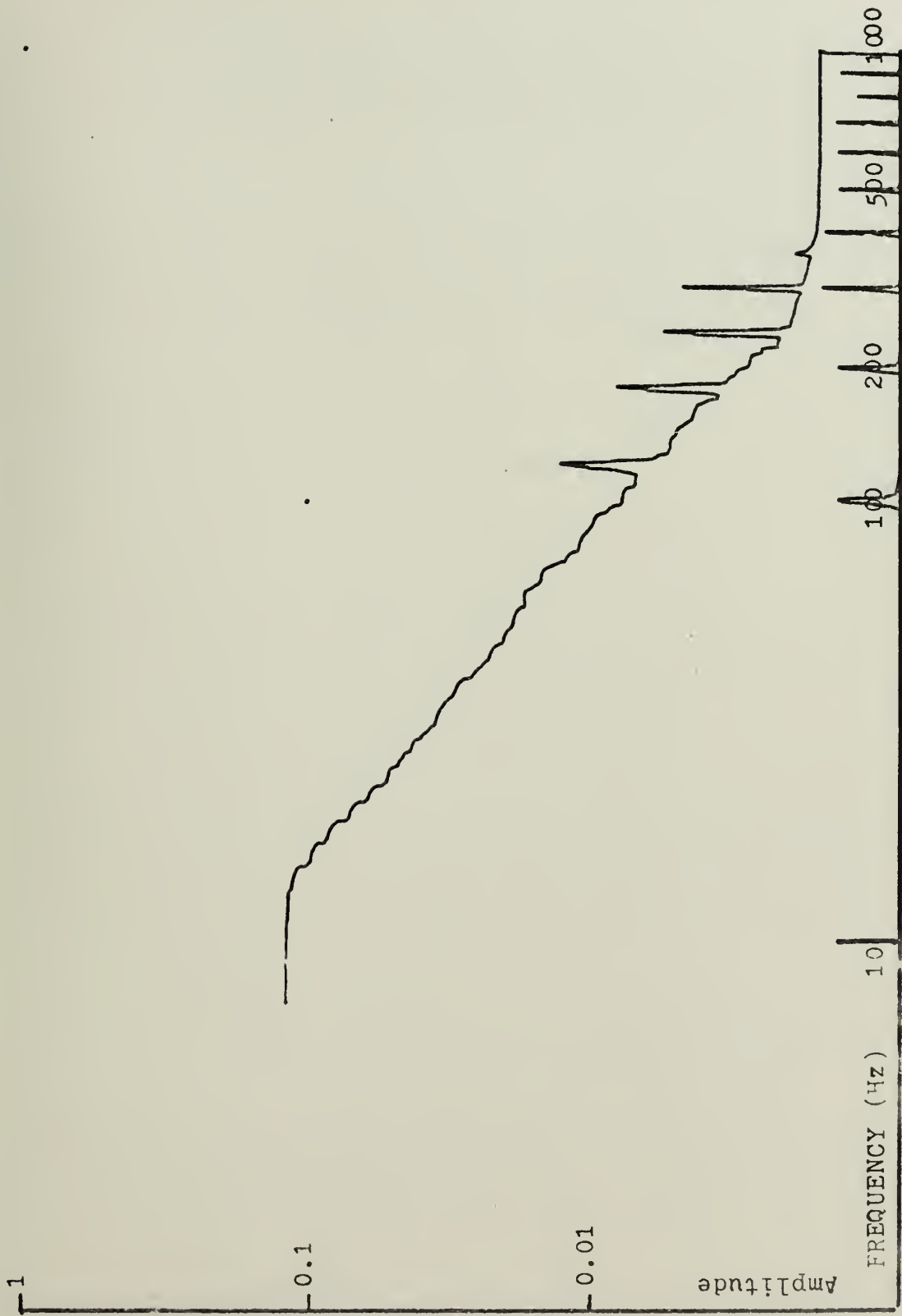


Fig. 27. Scintillation Spectrum: 0615





Fig. 28. Scintillation Spectrum: 0630





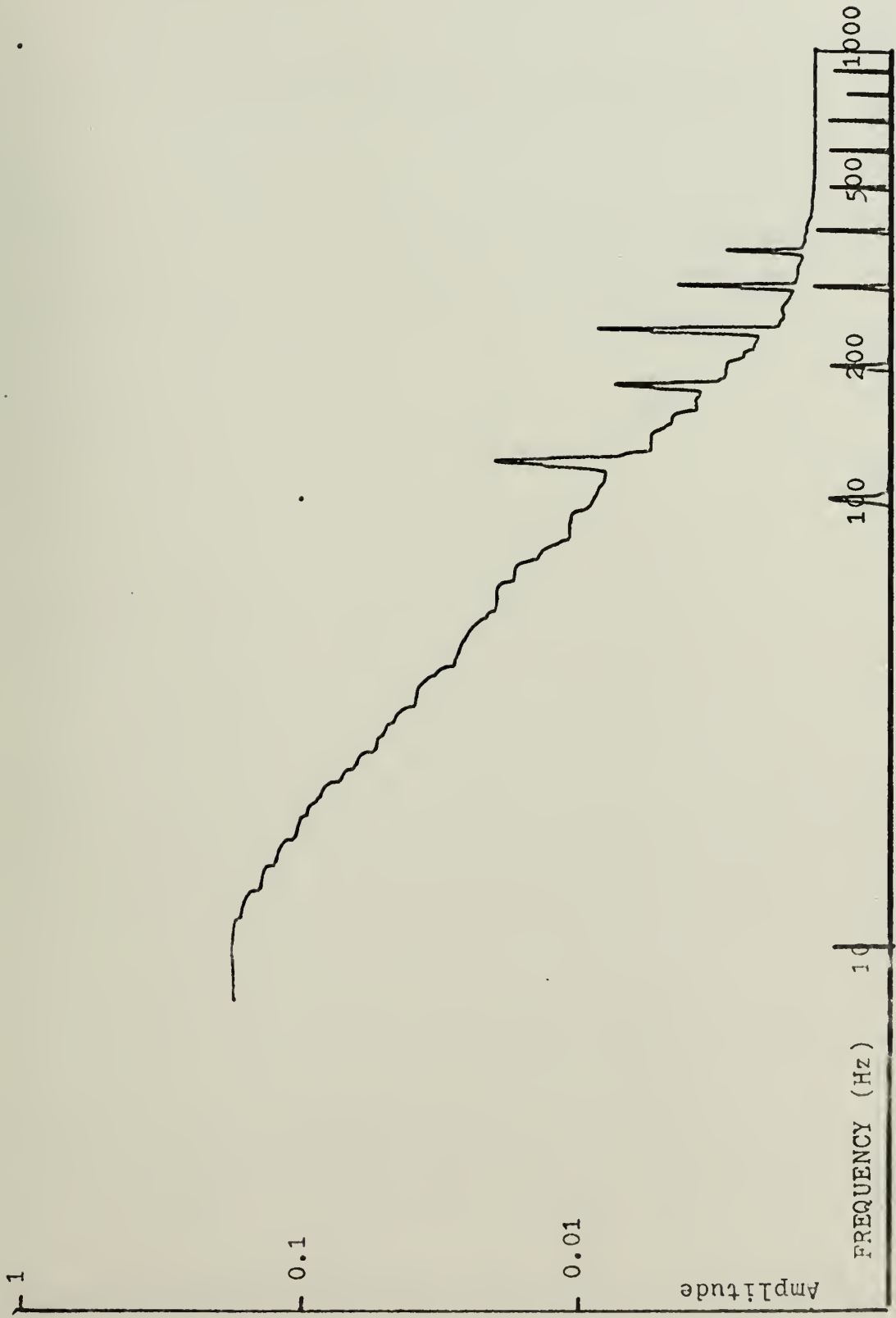


Fig. 29. Scintillation Spectrum: 0645



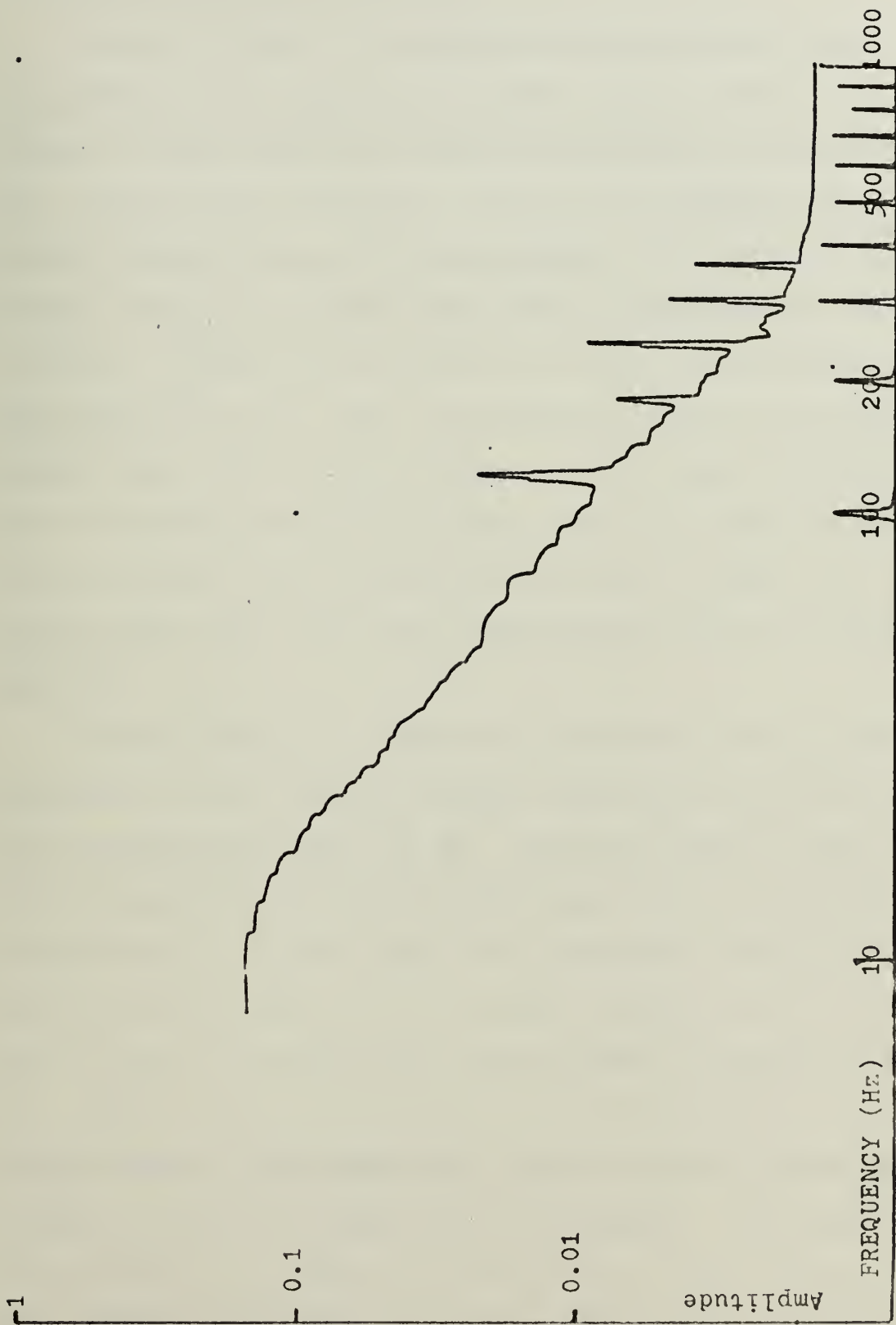


Fig. 30. Scintillation Spectrum: 0700



internal modulation circuitry.

Figure 31 shows a log-log plot of amplitude versus frequency of the amplified detector output (Point C of Figure 9) when the laser beam was modulated at 10 Hz with the electro-optic modulator. The 10 Hz component is just barely stronger than the scintillation. The high voltage ripple frequency (120 Hz) and several harmonics are readily visible. Figure 32 is a plot of the same 10 Hz modulation, this time using the direct modulation feature of the METRO-LOGIC laser. The 10 Hz component is even less distinguishable from the scintillation noise due to the lower modulation level achieved when modulating the laser in this way. A sixty hertz noise line and even harmonics are also clearly evident.

The multiplicative nature of the scintillation noise, as predicted by the theory, becomes very evident as the modulation frequencies reach 200 Hz. Figures 33 and 34 show the 200 Hz modulation by electro-optic and direct modulation, respectively. In both cases, the modulation has pulled the scintillation noise out to a higher frequency quite noticeably. This effect is dramatically demonstrated in Figures 35 and 36. Figure 35 is a plot of the scintillation alone (unmodulated laser) taken immediately before the plot shown in Figure 36, which is with 1000 Hz modulation. The basic scintillation in Figure 35 extends out to about 1000 Hz and when 1000 Hz modulation is applied (Figure 36) it is clear that the scintillation noise has been pulled out to about



200 Hz.

Figure 37 shows the spectrum with a modulating frequency of 5 kHz. Notice that at this frequency, the pulling of the scintillation noise sidebands around the modulated frequency is not as evident. The resolution limitations of the spectrum analyzer account for some of this, but the fact remains that the bandwidth of the 5 kHz line is less than the multiplicative model predicts.







Fig. 31. Modulation Spectrum: 10 Hz E/O Modulator



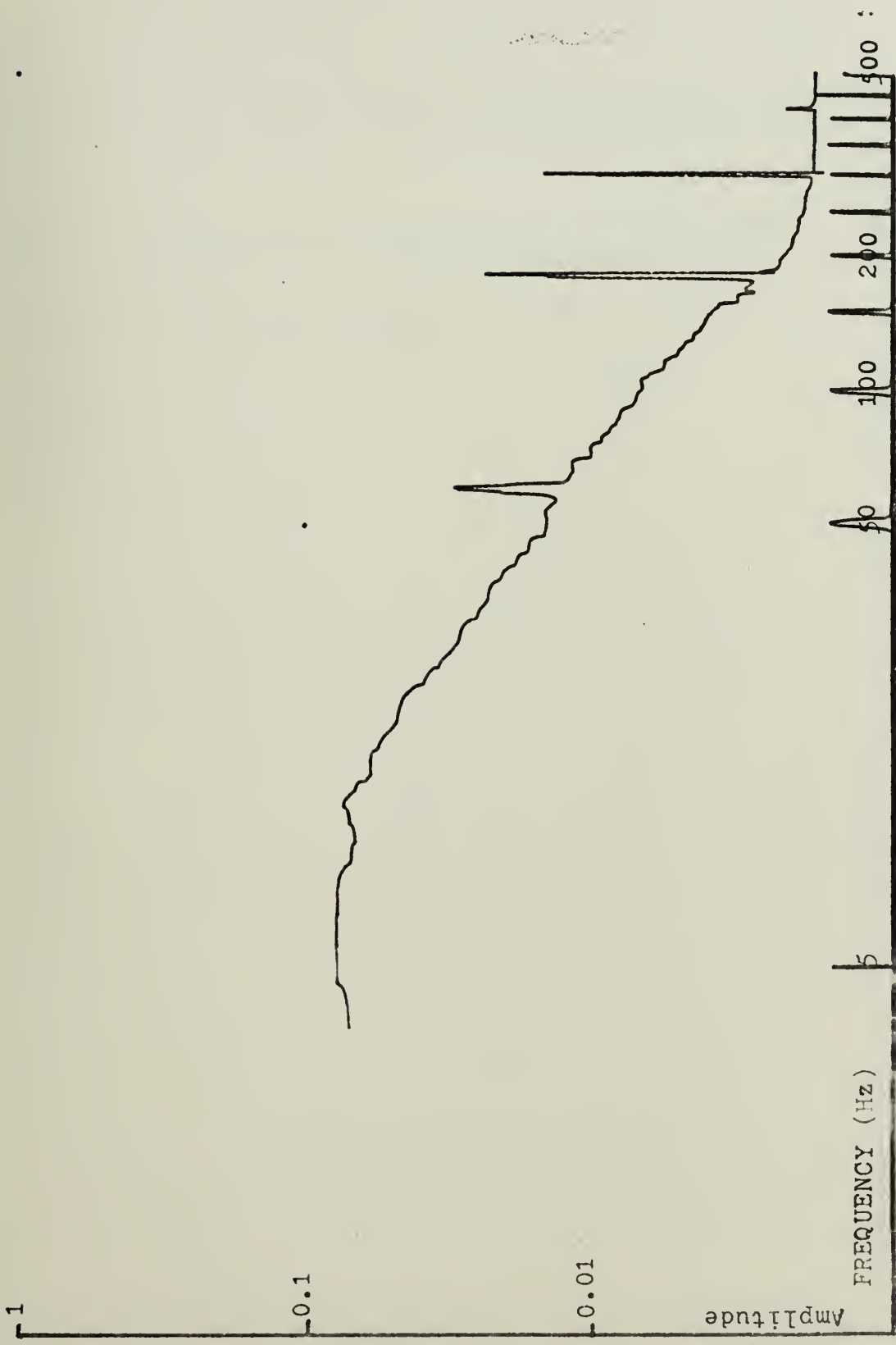


Fig. 32. Modulation Spectrum: 10 Hz Internal Modulator



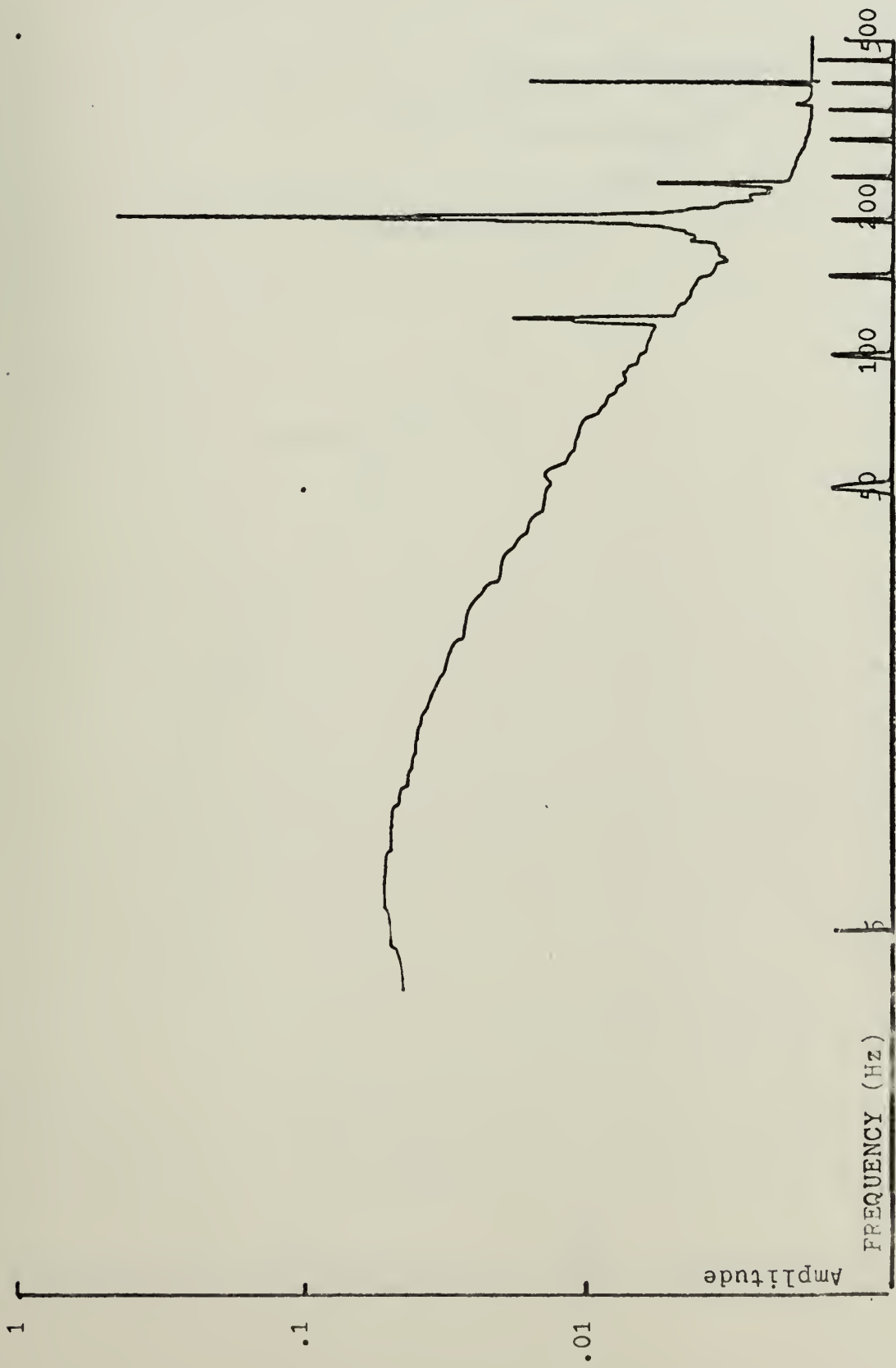


Fig. 33. Modulation Spectrum: 200 Hz E/O Modulator



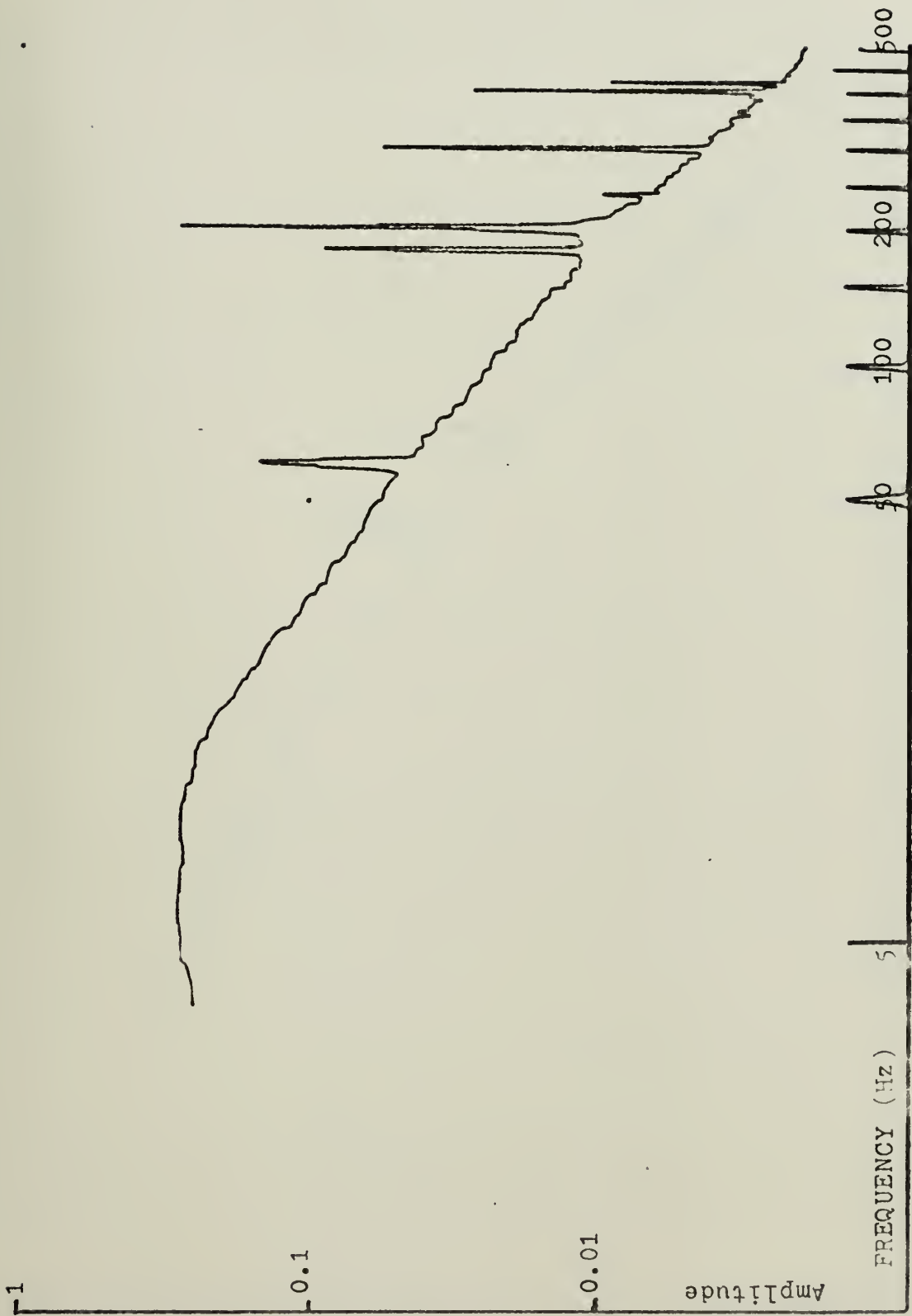


Fig. 34. Modulation Spectrum: 200 Hz Internal Modulator





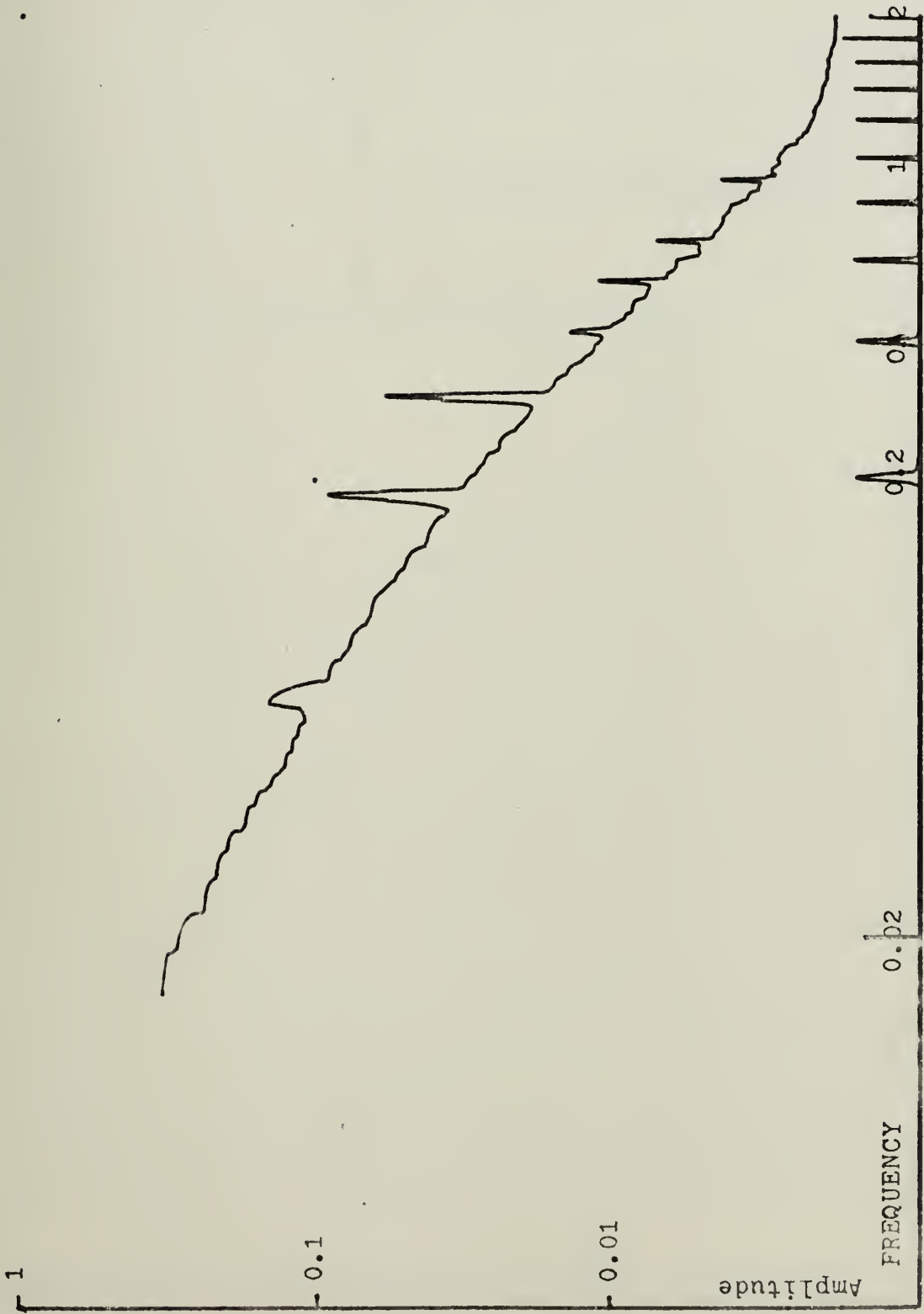


Fig. 35. Scintillation Spectrum: 0430



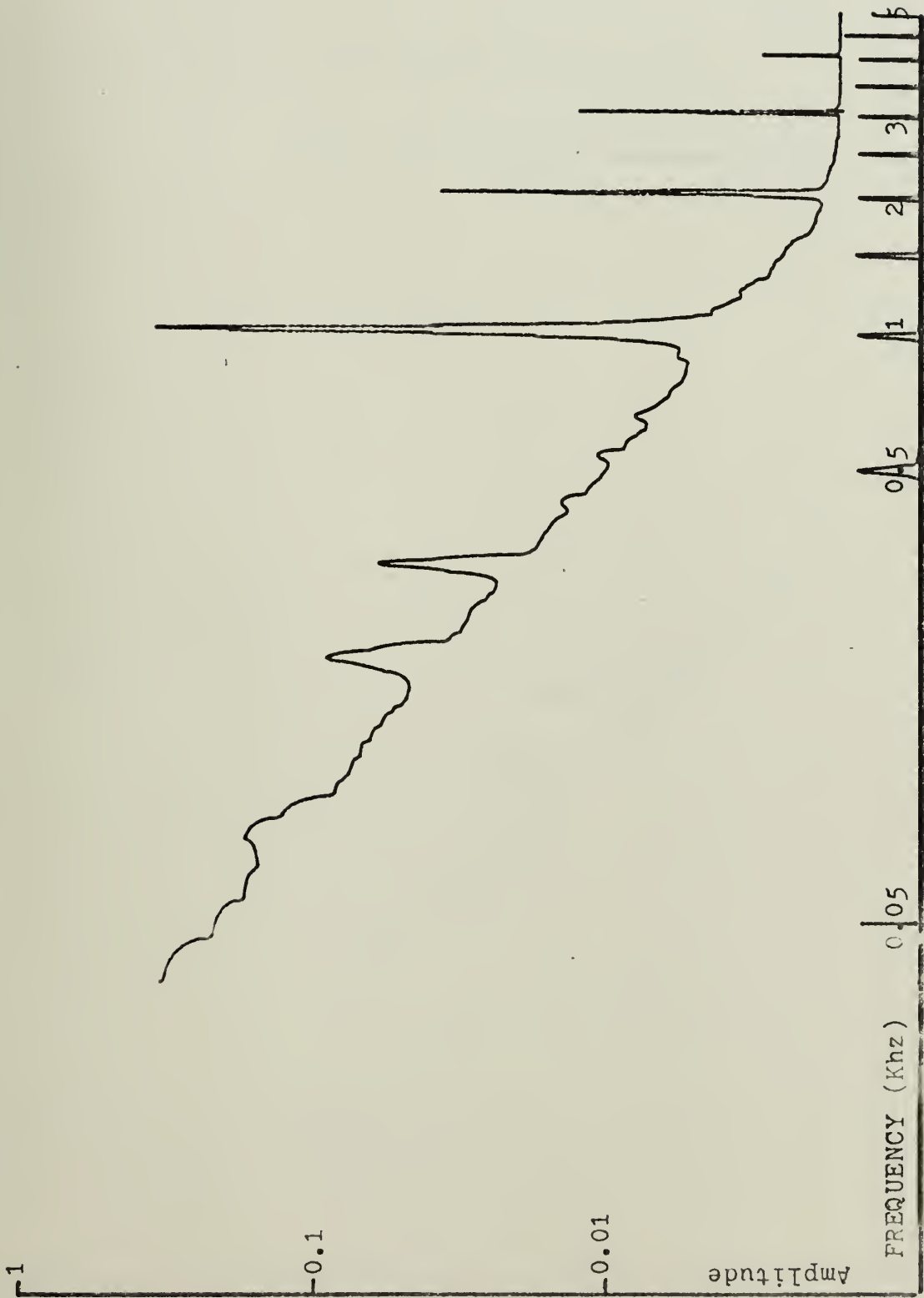


Fig. 36. Modulation Spectrum: 1 kHz



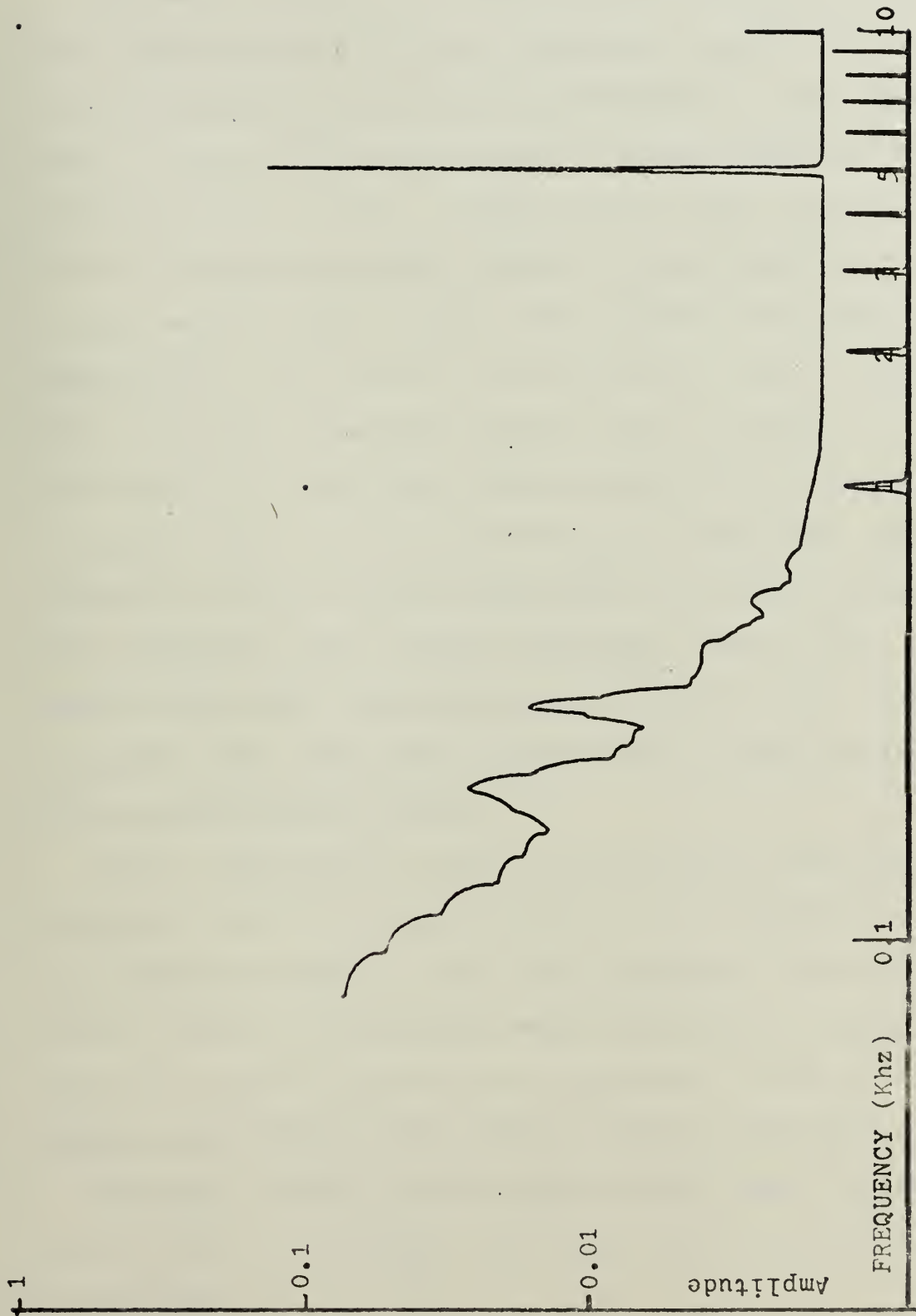


Fig. 37. Modulation Spectrum: 5 kHz



## VI. CONCLUSIONS

The model proposed by Rankin (Ref. 1) was not altered in this continuation of his work. Rankin's results were based on preliminary data and this continuation has made improvement on the data collection method and has collected a more extensive range of data. Looking at the data, however, it must be concluded that the validity of the predictive model is very much in doubt. That there exists a frequency translation effect, and hence, a multiplicative model of some kind, is readily apparant from the data in Chapter V, particularly at modulation frequencies in the vicinity of the upper limit of the raw scintillation spectrum. However, the model fails to predict accurately the bandwidth of the noise sidebands. The actual bandwidths observed are significantly less than predicted by equation (2). Thus, it appears that additional thought must be given to the form of the multiplicative model.

On the experimental side of the project, several improvements need to be made in order to be compatable with the shipboard project. First, and foremost, a detector with greatly improved sensitivity needs to be used. A high gain, low noise amplifier would be of assistance, however, the primary sensitivity of the detector must be improved.

Secondly, either a much higher quality tape recorder must be used or a portable, real time spectrum analyzer must be utilized.

In the signal processing area, a method should be found





to look more closely at the bandwidth of the detected signal with the higher modulation frequencies. A technique that would permit the examination of a "window" of frequency centered at the modulation frequency would be very useful in resolving the scintillation translation bandwidth question.

Lastly, more complex modulation waveforms should be tried. The use of a voice signal and/or some form of pulse code modulation could be tried. The data at higher modulation frequencies suggests that, due to less of the scintillation noise being pulled out to the higher frequencies, a baseband voice signal could be mixed to a higher frequency, (say 10 to 15 MHz) modulated onto the laser beam, received and detected, then translated back down to baseband. Similarly, pulse code modulation of some type could be tried to determine the actual effects of scintillation noise on error rates.



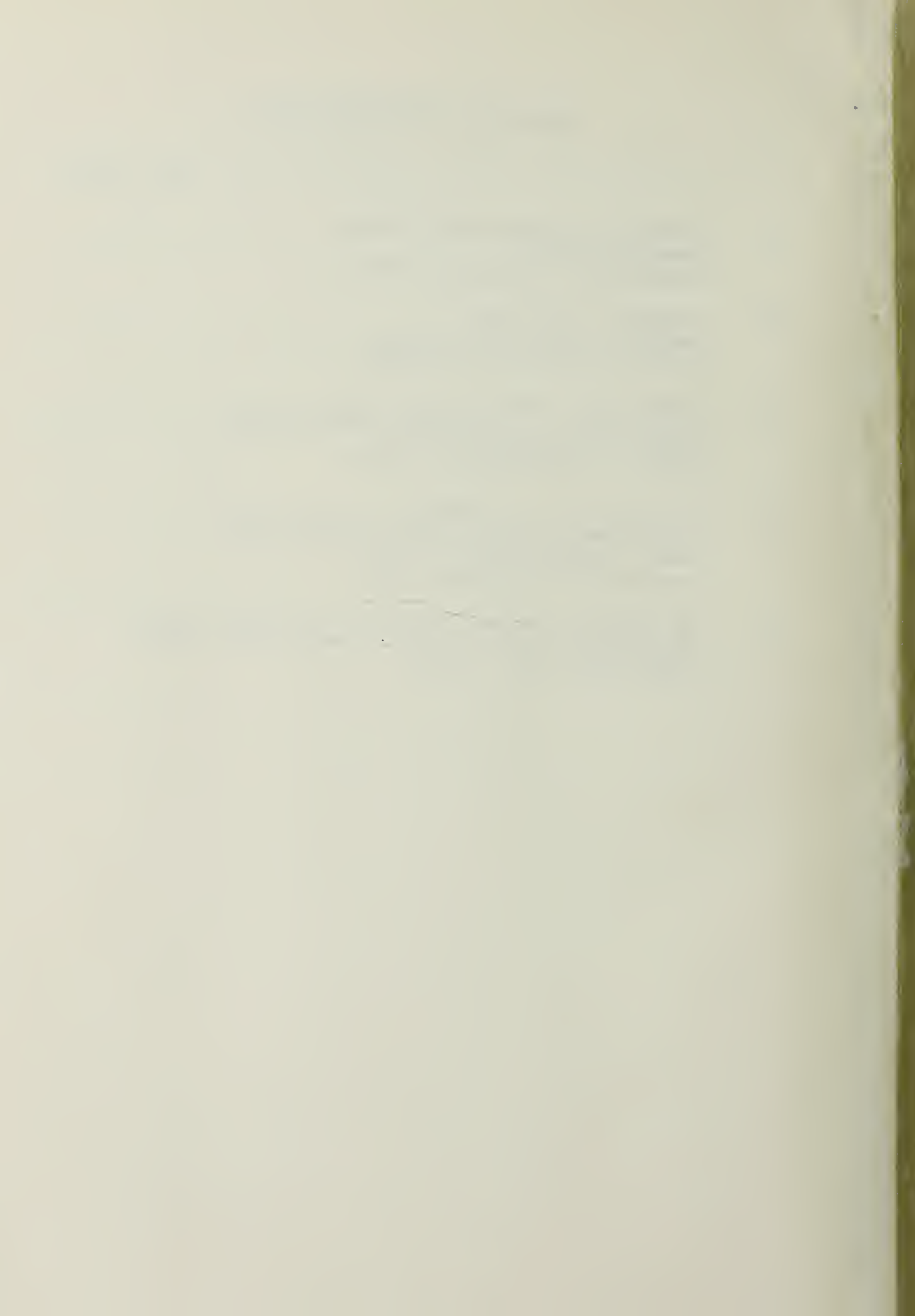
## LIST OF REFERENCES

1. Rankin, T.P., Effects of Atmospheric Turbulence on Laser Communications, Master's Thesis, Naval Post-graduate School, Monterey, Ca., June, 1974.
2. Lumley, J.L., Panofsky, H.A., The Structure of Atmospheric Turbulence, Interscience Monographs, Wiley and Sons, New York, 1964.
3. Tatarski, V.I., trans. by Silverman, R.A., Wave Propagation in a Turbulent Medium, McGraw-Hill Book Company, Inc., New York, 1961.
4. Schmeltzer, R.A., Means, Variances and Covariances for Laser Beam Propagation Through a Random Medium, North American Aviation E.O. Lab, December, 1965.
5. Fried, D.L., "Propagation of a Special Wave in a Turbulent Medium", Journal of the Optical Society of America, Vol. 57, No. 2, February, 1967.
6. Fried, D.L., Seidman, J.B., "Laser Beam Scintillation in the Atmosphere", Journal of the Optical Society of America, Vol. 57, No. 2, February, 1967.



## INITIAL DISTRIBUTION LIST

		No. Copies
1.	Defense Documentation Center Cameron Station Alexandria, Virginia 22314	2
2.	Library, Code 0212 Naval Postgraduate School Monterey, California 93940	2
3.	Department Chairman, Code 52 Department of Electrical Engineering Naval Postgraduate School Monterey, California 93940	2
4.	Professor C.H. Rothage Department of Electrical Engineering Naval Postgraduate School Monterey, California 93940	1
5.	Lt. Tadd E. Spicer, USN Naval Electronics System Command (PME 106-5) Washington D.C. 20360	1



Thesis  
S6683 Spicer  
c.1

156605

Atmospheric turbulence  
effects on laser communi-  
cations systems.

Thesis  
S6683 Spicer  
c.1

156605

Atmospheric turbulence  
effects on laser communi-  
cations systems.

thes56683

Atmospheric turbulence effects of laser



3 2768 001 00763 6

DUDLEY KNOX LIBRARY